INHERENT ANTIBACTERIAL ACTIVITY OF A B-HAIRPIN PEPTIDE HYDROGEL: THE EFFECT OF THE LYSINE SIDE CHAIN LENGTH ON ANTIBACTERIAL ACTIVITY

by

Heather Ann Hartman

A thesis submitted to the Faculty of the University of Delaware in partial fulfillment of the requirements for the degree of Honors Bachelor of Science in Chemistry with Distinction.

Spring 2010

INHERENT ANTIBACTERIAL ACTIVITY

OF A B-HAIRPIN PEPTIDE HYDROGEL:

THE EFFECT OF THE LYSINE SIDE CHAIN

LENGTH ON ANTIBACTERIAL ACTIVITY

by

Heather Ann Hartman

Approved: _____

Joel P. Schneider, Ph.D.
Professor in charge of thesis on behalf of the Advisory Committee

Approved: _____

Neal Zondlo, Ph.D.
Committee member from the Department of Chemistry and Biochemistry

Approved: _____

Sherry Kitto, Ph.D.
Committee member from the Board of Senior Thesis Readers

Approved: _____

Alan Fox, Ph.D.
Director, University Honors Program

ACKNOWLEDGMENTS

This thesis was only possible with the help of others. I would like to thank Dr. Joel P. Schneider and the Schneider group for letting me work in their lab, attending group meetings, and for all the help and advice they provided. I would especially like to thank Dr. Daphne Salick and Dr. Monica Branco for teaching me everything I know and supporting me in the lab. In addition, I would like to thank the Undergraduate Research Program and my thesis committee (Dr. Schneider, Dr. Zondlo, and Dr. Kitto) for administrative help and advice. Finally, I would not have survived this project without the love and support of my family and friends.

TABLE OF CONTENTS

LIST OF FIGURES

ABSTRACT

Self-assembling peptide hydrogel scaffolds have the potential for use in tissue regenerative therapies. Hydrogels provide an ideal, hydrated, porous environment for tissue growth. However, for the implantation of a biomaterial, many design considerations and precautions must be met, in particular preventing the introduction of infection. A lysine-rich peptide, MAX1, has been designed so that it self-assembles upon the addition of a trigger, forming a hydrogel whose surface is active against Gram-positive (*Staphylococcus epidermidis*, *Staphylococcus aureus* and *Streptococcus pyogenes*) and Gram-negative (*Klebsiella pneumoniae* and *Escherichia coli*) bacteria, all prevalent in hospital settings. Although detrimental towards bacteria, the surface is cytocompatible towards a variety of mammalian cells, making these hydrogels attractive candidates as tissue engineering scaffolds. Although it is known that MAX1 hydrogels demonstrate antibacterial properties, the mechanism for this behavior is not understood. This research focused on determining the effect of the length of the lysine side chains of MAX1 on the material properties as well as the antibacterial activity of the hydrogel surface. Two new peptide sequences, HPL1 and HPL2, were designed, in which the lysine residues were homogenously replaced by ornithine, a methylene deficient derivative of lysine, and diaminobutyric acid, a di-methylene deficient derivative of lysine, respectively. Only HPL1 was studied beyond synthesis and purification because HPL2 failed to form a rigid hydrogel. In order to assess the physical properties of the peptide hydrogels, the storage and loss moduli were measured using oscillatory shear rheology and the mean residue ellipticity was

measured using circular dichroism spectroscopy. The results were compared to those of MAX1 hydrogels. Additionally, soluble HPL1 and HPL1 hydrogels were challenged with *Staphylococcus aureus* and *Escherichia coli* in order to determine the antibacterial activity of the soluble peptide and peptide hydrogel. The HPL1 hydrogels demonstrated reduced efficacy against *S.aureus* when compared to the MAX1 hydrogels, and the soluble peptide continued to show no activity. However, the HPL1 hydrogels showed increased inhibition against *E.coli*. The same results were observed for the soluble HPL1. This research provides some insight into the mechanism of antibacterial activity for hydrogels of MAX1 and its derivatives.

Chapter 1

INTRODUCTION

1.1 Introduction to Hydrogels and Their Biomedical Applications

Within the last twenty years, hydrogels have become a type of polymer with significant promise in the medical industry. Among the current applications of hydrogels on the market, hydrogels are found as wound-healing bioadhesives, contact lenses, sustained release drug delivery systems, and tissue reengineering scaffolds (13). Hydrogels are cross-linked polymeric structures with a very high water content that have both liquid and solid characteristics. The water content must be at least 20% of the total weight, and are considered superabsorbent if the water content is at least 95% of the total weight (10). The physical properties of hydrogels are determined by the polymer network and the absorbency of that network. When the appropriate polymer network is used, hydrogels can have both an elasticity and a rigidity, or storage modulus, similar to that of natural tissues. Therefore, hydrogels can be designed to have specific storage modulus. Additionally, hydrogels are typically biocompatible and frequently biodegradable (3).

Since tissue engineering, in the most general of senses, seeks to fabricate living replacements for parts of the body, hydrogels stand as ideal potential scaffolds. Hydrogels can be designed to closely match a tissue of interest and the specific application. One of the most widely used hydrogels as a biological material is poly(hydroxyethylmethacrylate) (PHEMA) (13). Both naturally derived and synthetic

materials exist for use in forming hydrogels, including agarose, chitosan, collagen, and hyaluronic acid (HA) for natural options and poly(ethylene oxide) (PEO), poly(vinyl alcohol) (PVA), poly(propylene fumarate-co-ethylene glycol) (PEG), and polypeptides as synthetic materials (4). Naturally derived materials are typically used because they have properties similar to the natural extracellular matrix (ECM). By comparison, synthetic materials are ideal for tissue engineering materials because their properties are able to be controlled and are reliably reproduced. Each of these hydrogels serves its purpose within the tissue engineering community due to its unique properties.

Many challenges exist for hydrogels that are introduced into the human body. First and foremost, the hydrogel must be biocompatible and cytocompatible; it cannot illicit an immune response, kill the surrounding tissue, or be rejected from the body (13). The degree of biocompatibility and cytocompatibility needed for a specific hydrogel is dependent upon its intended application. Additionally, it is advantageous for a hydrogel to be biodegradable (3). It is therefore important to choose polymers made of bonds that can be degraded under physiological conditions, such as enzymatic or chemical hydrolysis, when designing a hydrogel for most biomedical applications. The hydrogel must also exhibit physical properties similar to the tissue that is being replaced (4). While hydrogels can be designed to meet each of these requirements, there exists another problem with them. Hydrogel materials typically provide a suitable environment for host cell function. However, the warm, moist environment provided by these materials also offers an ideal site for opportunistic bacteria (15). In order to address this concern, hydrogels have been designed that encapsulate antimicrobial agents or that have antimicrobial agents covalently attached to the

polymeric scaffold (7). Therefore, there are many considerations that must be taken into account when designing a hydrogel polymer for biomedical application.

1.2 Introduction to Antibacterial Peptides

While the first understanding and application of antibiotics by humans occurred over a century ago, nature has made and used antibacterial, and more generally antimicrobial, substances for a much longer period of time. The discovery of naturally occurring antimicrobial molecules has led to the development of many synthetic antimicrobial pharmaceuticals. Within the classes of antibiotics, there are several that are peptide-derived including antimicrobial peptides (AMPs), glycopeptides, streptogramins, and cyclic peptides (9, 17). Most of these antibiotics are selective to either Gram-positive bacteria or Gram-negative bacteria. Those that are antibacterial against both types of bacteria typically are more effective against one class (1). The difference in efficacy is explained by the variety of antibacterial mechanisms of action classes, including inhibition of the bacterial cell wall biosynthesis, inhibition of protein synthesis, cell membrane disruption, and inhibition of nucleic acid synthesis (9). With such a large variety of antimicrobial peptides and classes of action, antimicrobial peptides present significant opportunity for the development of novel pharmaceuticals that are highly specialized.

Of recent interest is the class of AMPs, which shows potential for development as antibiotics, antifungal agents, antiprotozoa agents, and cancer treatments. These molecules are an evolutionarily conserved component of the innate immune response. AMPs, also known as cationic peptides, are generally defined as peptides that contain less than 100 amino acid residues and that possess the amphiphilic characteristics of an overall positive charge and a substantial hydrophobic

region (5). While there are a variety of secondary structures including α-helices, parallel and anti-parallel ß-sheets, loops, and extended peptides for AMPs, the hydrophobic and hydrophilic regions are thought to be ideal for interacting with the membrane interface (5, 6, 18). However, there is disagreement over the mechanism of action for this class of peptide. Some cationic peptides influence macromolecular synthesis without breaking down the membrane, others lodge within the membrane, and finally others permeabilize the cytoplasmic membrane (6). While peptides are not delivered orally due to the enzymes in the digestive system, other methods of delivery, such as intravenous injection and implantation, exist. Even when delivered intravenously or by implantation, antimicrobial peptides will eventually degrade due to proteases found throughout the body. The rate at which these peptides degrade depends on their composition; therefore AMPs can be designed for specific biodegradation rates. Using natural AMPs as a design model, many synthetic variants have and continue to be designed.

1.3 Introduction to MAX1

The potential of antimicrobial peptide hydrogels as scaffolds for tissue reengineering and drug delivery presents the opportunity for significant growth within the scientific and medical communities. Small peptides have been designed to take advantage of the physical and biological properties of AMPs. One such peptide, MAX1, consists of two ß-strands of alternating valine and lysine residues between a tetrapeptide sequence (-V^{D}PPT-), as shown in Figure 1.1 (16). The tetrapeptide sequence was designed to form a type II' ß-turn under specific conditions. Additionally, the alternating polar and nonpolar residues on either side of the ß-turn were designed to form a ß-hairpin state upon self-assembly.

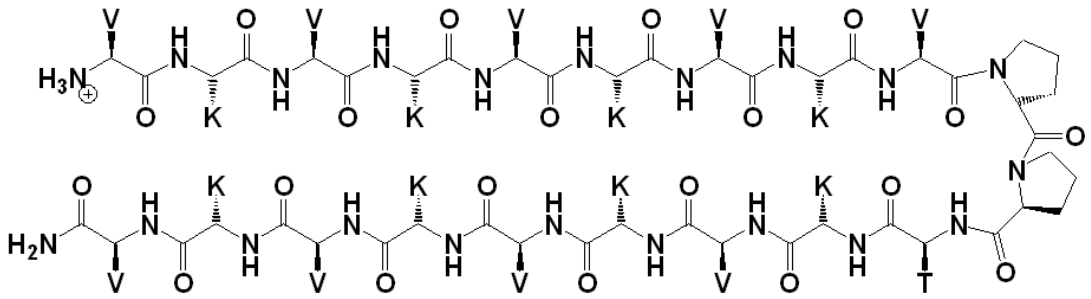

MAX1: VKVKVKVKV^{D}PPTKVKVKVKV-NH_2

Figure 1.1 The sequence of MAX1 with the ß-turn shown.

Figure 1.2 depicts the folding and self assembly of MAX1 upon the addition of a folding trigger (11). The folding and self-assembly of MAX1 is triggered by the introduction of a variety of conditions including high pH, salt, temperature, and cell culture media (8, 11, 12, 16). Upon folding into a ß-hairpin, one face of the hairpin consists of the hydrophilic lysine side chains and the other face consists of the hydrophobic valine side chains. Self-assembly of the facially amphiphilic peptide is driven by facial hydrophobic interactions and lateral intramolecular hydrogel bonding. The self-assembled peptide hydrogel has significant ß-sheet formation as determined by circular dichroism (11, 16). Depending on the specific trigger used to initiate folding and self-assembly, MAX1 hydrogels can have a variety of storage moduli.

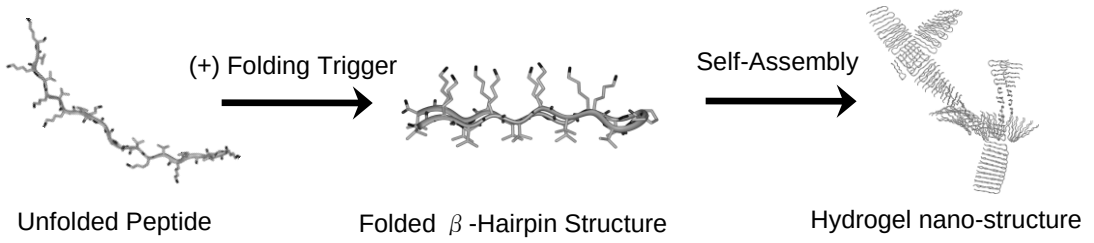

Figure 1.2 The mechanism for folding and self-assembly of MAX1 into a hydrogel state.

In order for a hydrogel to be used within the human body for tissue engineering scaffolds, it must be proven to be cytocompatible and biocompatible. The hydrogel cannot cause cells to die, it must allow cells to proliferate in its presence, and it cannot illicit an immune response (4). Additionally, in the presence of the desired cells, the hydrogel must be mechanically rigid and able to support the stress of that location (2). Preliminary results indicate that MAX1 hydrogels are mechanically rigid in cell culture conditions, are non-toxic towards model fibroblasts, and encourage the attachment and proliferation of the model fibroblast cells (8). Furthermore, the *in vitro* pro-inflammatory potential was assessed for MAX1 hydrogels. The studies showed that MAX1 hydrogels illicit minimal secretions of the inflammatory response molecule TNF-α and the macrophages under study remain in their inactivated state (14). Therefore, preliminary studies demonstrated that MAX1 hydrogels are both cytocompatible and biocompatible.

Another concern for tissue engineering scaffolds and other biomaterials is the risk of the introduction of infection. While many hydrogel materials have addressed this problem by incorporating antimicrobial agents within the gel, MAX1

hydrogels were discovered to be inherently antibacterial. MAX1 hydrogels were challenged with Gram-positive and Gram-negative bacteria species in order to study this desired property. Figure 1.3 depicts the antibacterial activity of tissue culture treated polystyrene (TCTP) control surfaces and 2wt% MAX1 hydrogel surfaces challenged with increasing numbers colony forming units (CFUs) of Gram-positive *Staphylococcus aureus* (15). After being challenged with *S.aureus* for 48 hours, the 2wt% MAX1 surface showed that it inhibited the proliferation of up to 2×10^{9}CFU/dm^{2}. The TCTP control surfaces allowed proliferation of even the smaller numbers of bacteria. Similar results were obtained for Gram-positive species *Staphylococcus epidermidis* and *Streptococcus pyogenes*, demonstrating that 2wt% MAX1 hydrogels inhibit the growth of Gram-positive species.

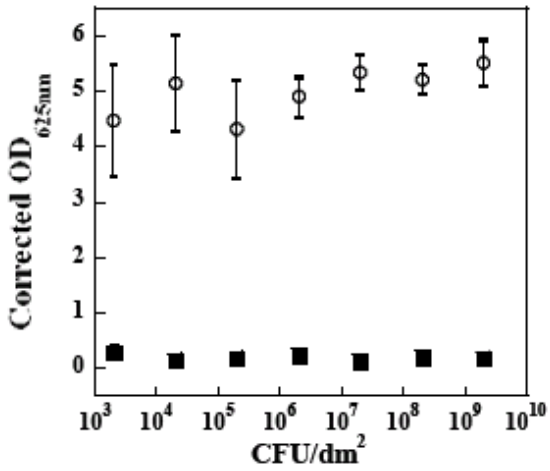

Figure 1.3 Tissue Culture Treated Polystyrene control surfaces and 2wt% MAX1 hydrogel surfaces challenged with increasing numbers of CFUs of Gram-positive *Staphylococcus aureus* for 48 hours. Open, round points represent TCTP surfaces and closed, square points represent 2wt% MAX1 hydrogel surfaces.

Similar assays were performed for Gram-negative *Escherichia coli* for 24 and 48 hours (15). The results are depicted in Figure 1.4. After just 24 hours, 2wt% MAX1 hydrogels inhibits bacterial proliferation of up to 2×10^8 CFU/dm^2. The inhibitory activity of the surface decreases when the surface is challenged for 48 hours and the gel inhibits proliferation of up to 2×10^6 CFU/dm^2. For another Gram-negative species, *Klebsiella pneumoniae*, the inhibitory activity after 48 hours was similar to that of *E.coli* after 24 hours. While the 2wt% MAX1 hydrogels show a decrease in the antibacterial activity for Gram-negative species when compared to Gram-positive species, the hydrogel surface offers effective antibacterial activity against the levels of bacteria that are acceptable within an operating theater (15). Live-dead laser scanning confocal microscopy studies of the surfaces showed that the proliferation inhibition was due to the bacteriocidal nature of the 2wt% MAX1 hydrogel.

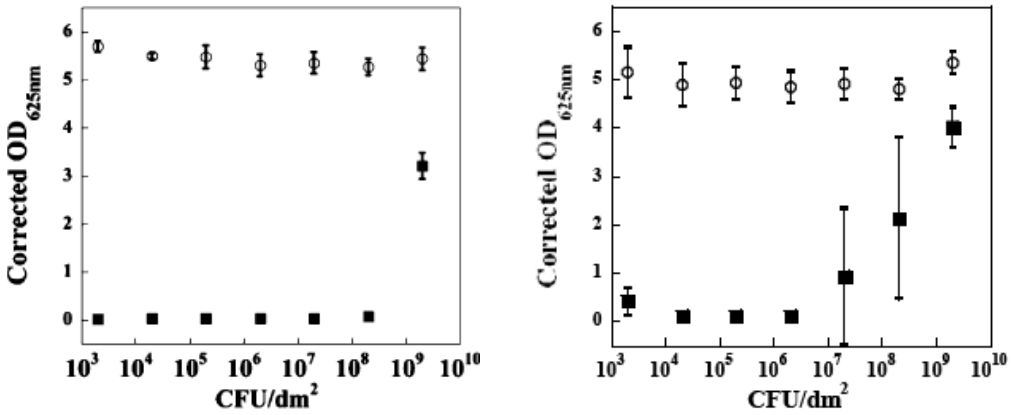

Figure 1.4 Tissue Culture Treated Polystyrene control surfaces and 2wt% MAX1 hydrogel surfaces challenged with increasing numbers of CFUs of Gram-negative *Staphylococcus aureus* for 24 hours (left) and 48 hours (right). Open, round points represent TCTP surfaces and closed, square points represent 2wt% MAX1 hydrogel surfaces.

While most of the peptide is incorporated into the hydrogel, some folded MAX1 remains in solution and is capable of forming aggregates. It is possible that these aggregates, and not the hydrogel, are the source of the antibacterial activity. Soluble peptide studies were performed using *S.aureus* and *E.coli*. Figure 1.5 presents the results of the soluble peptide study (15). The soluble peptide displays no antibacterial activity for both the Gram-positive and the Gram-negative species. Therefore it can be concluded that the inhibitory effect is due to the 2wt% MAX1 hydrogels and not the soluble peptide. In order to understand the bacteriocidal behavior of the 2wt% MAX1 hydrogel and its mechanism of action, a bacterial membrane disruption study was performed. This study showed that *E.coli* in the presence of 2wt% MAX1 released cytoplasmic ß-galactosidase, demonstrating that the membrane was lysed by MAX1 (15). However, it is unclear whether the lysis of the membrane caused bacterial death or the bacterial death resulted in the lysis of the membranes.

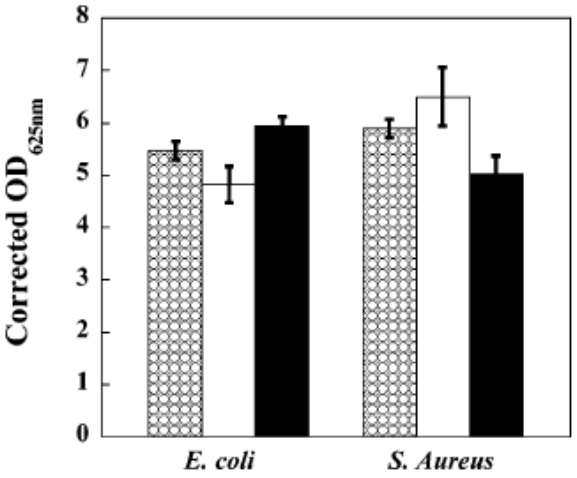

Figure 1.5 Proliferation of 2×10^6 CFU/dm^2 *E.coli* and *S.aureus* on control TCTP surfaces in the absence (checked) and presence (white) of 100µM MAX1, and in the presence of 38.7mM TFA (black).

1.4 Derivatives of MAX1

More information is needed to understand the mechanism of action of MAX1. It is unclear what the active component of the peptide hydrogel is. As was mentioned previously, large cationic charge is known to be the source of antimicrobial activity in many AMPs like MAX1. However, it is unclear whether the lysine side chain length plays a role in the antimicrobial activity of MAX1. One possibility is that the lysines on the beta sheets form a blanket of positive charge and it is this blanket that causes the antibacterial activity. Another possibility is that each side chain individually works to tunnel into the bacterial membrane. In both cases, the distance of the amine groups from the beta sheets might have an effect on the antimicrobial activity of MAX1. A combination of both these answers is also possible. In order to solely study the effect of the lysine side chains, the placement of ornithine (HPL1) and diaminobutyric acid (HPL2) for each lysine in the MAX1 sequence was proposed. Figure 1.6 depicts the physical differences between lysine, ornithine, and diaminobutyric acid. The general structure of the derivatives is also shown.

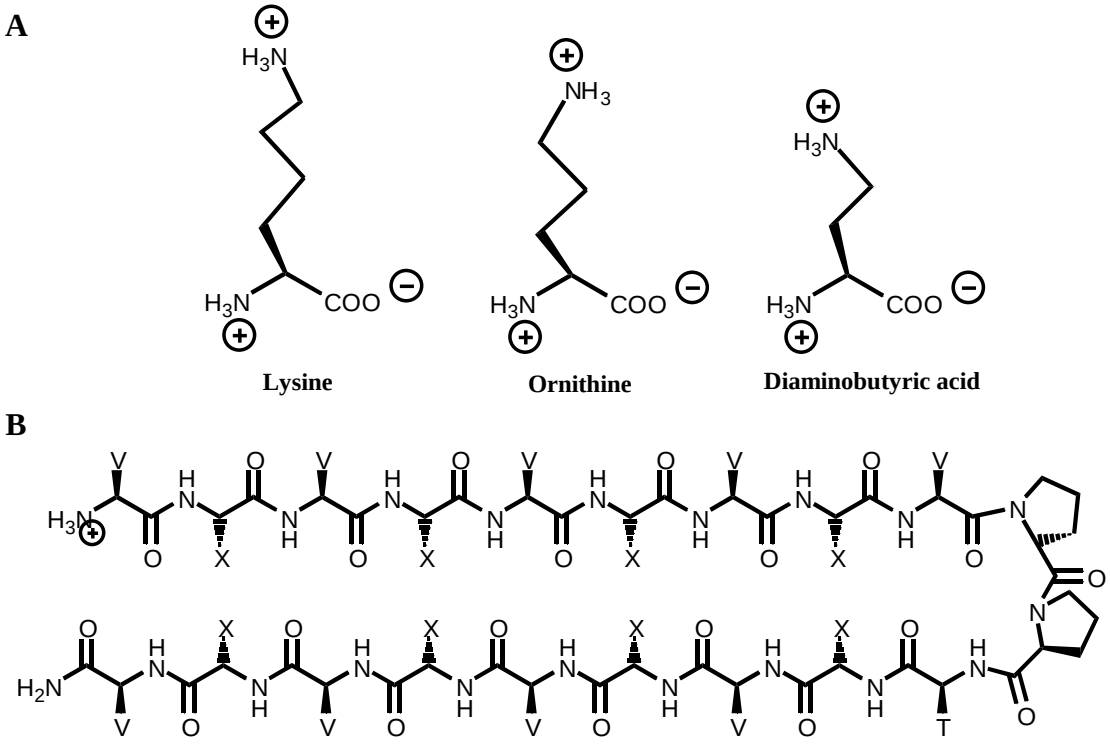

Figure 1.6 The structures of lysine, ornithine, and diaminobutyric acid (A), demonstrating the decrease in methylene in the side chain. The general structure for MAX1 and its derivatives (B) where lysine (MAX1), ornithine (HPL1), or diaminobutyric acid (HPL2) is located at each X in the peptide sequence.

Ornithine and diaminobutyric acid are unnatural derivatives of lysine, where the side chain has been shortened by one and two methylene groups, respectively. The study of HPL1 and HPL2 will examine how the shorted side chains effects the antibacterial properties of the hydrogel. Additionally, the rheological and secondary structure properties will be studied. In theory, the side chain could possibly be used to push or tunnel through the outer layers of bacterial membranes to introduce the positively charged amine group to the inside of the membrane, facilitating the

disruption and death of bacteria. The results will be used to understand if and how the lysine side chain plays a role in the antibacterial activity of MAX1.

Chapter 2

PEPTIDE SYNTHESES AND PURIFICATIONS

2.1 Introduction

As previously described, MAX1 is a twenty amino acid sequence composed of alternating valine and lysine amino acids with a D- and L-proline at positions nine and ten, respectively, and threonine at position eleven. Replacement of lysine in MAX1 with ornithine and diaminobutyric acid yielded the derivative peptides HPL1 and HPL2. The following syntheses and purifications were conducted in order to perform future studies. For each peptide purity was determined by analytical Reverse Phase High Performance Liquid Chromatography (RP-HPLC) and electrospray ionization mass spectrometry (ESI-MS).

2.2 Materials and Methods

2.2.1 Materials

The PL-Rink amide resin was purchased from Polymer Laboratories. Fmoc (fluorenylmethyloxycarbonylchloride)-protected amino acids were purchased from Synpep, except for Fmoc-Ornithine(Boc)-OH and Fmoc-Diaminobutyric acid(Boc)-OH, which were purchased from Novabiochem. The 1H-Benzotriazolium 1-[*bis*(dimethylamino) methylene]-5chloro-hexafluorophosphate (1-),3-oxide (HCTU) was purchased from Peptides International. Trifluoroacetic acid (TFA), thioanisole,

ethanedithiol, and anisole were purchased from Acros. Diethyl ether, methanol, and acetonitrile were purchased from Fischer Scientific.

2.2.2 Peptide Synthesis

The peptides that were prepared were MAX1, HPL1, and HPL2. Peptides were prepared on PL-Rink amide resin from Polymer Laboratories via an automated ABI 433A peptide synthesizer employing standard Fmoc protocol and HCTU activation in 0.25mmole and 1.00mmole batches. The C-terminal was aminated in each peptide. The resulting dry resin-bound peptides were cleaved and the side-chains deprotected using a cleavage cocktail of TFA, thioanisole, ethanedithiol, and anisole in a ratio of 90:5:3:2 for two hours under a nitrogen atmosphere. The solution was filtered to remove the resin and the peptide was precipitated from the filtrate using cold ethyl ether, affording the crude peptide.

2.2.3 Peptide Purification

Crude peptide was purified by RP-HPLC on a preparative Vydac C18 peptide/protein column at 40^{o}C with a gradient of 0% to 0% B over 2 minutes, then a linear gradient from 0% to 15% over the next 4 minutes, then 15% to 100% over 170 minutes, where A is 0.1% TFA in water and B is 90% acetonitrile, 9.9% water, 0.1% TFA. A flow rate of 8mL/min was used in the preparative HPLC. The peptides eluted at 31 minutes. The resulting peptide solutions were frozen in liquid nitrogen and lyophilized to obtain the pure peptide as the TFA salt. ESI-MS and analytical RP-HPLC of the peptides were taken to confirm peptide purity and identity. For the analytical RP-HPLC, a gradient of 0% to 100%B over 100 minutes was used at a flow

rate of 1mL/min. The analytical Vydac C18 peptide/protein column was kept at 20°C. The peptides eluted at 28 minutes.

2.3 Results and Discussion

2.3.1 MAX1 Synthesis and Purification

The purified, lyophilized MAX1 peptide was a fluffy white powder. A sample of the peptide was analyzed using analytical RP-HPLC to ensure its purity. A gradually increasing absorbance at 220nm with a single, sharp peak at 28 minutes indicated a pure sample with a polarity of MAX1. Figure 2.1 shows a representative RP-HPLC spectrum of pure MAX1 peptide. Note the lack of pre- and post-peaks around the peak at 28 minutes.

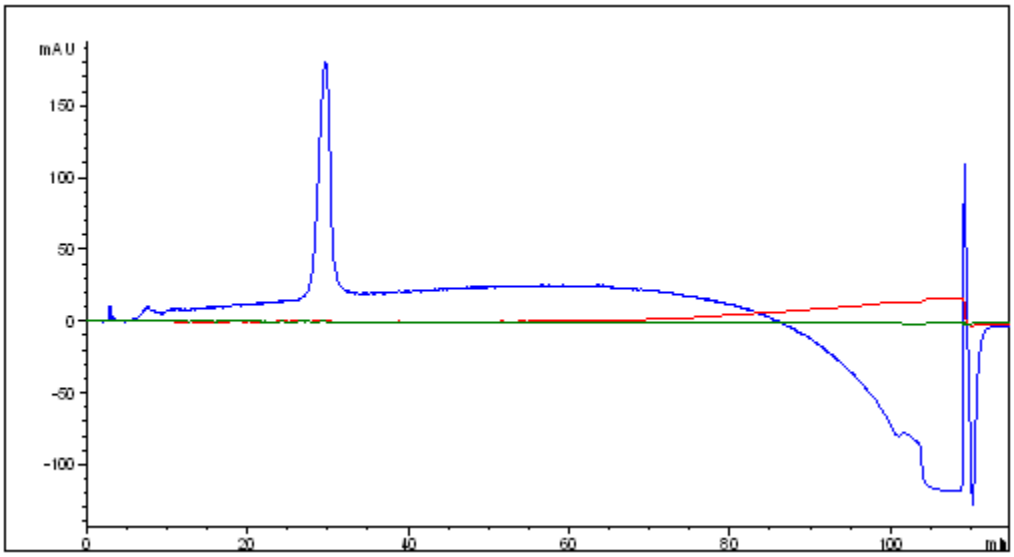

Figure 2.1 Analytical RP-HPLC of pure MAX1 in methanol. MAX1 eluted at 28 minutes.

While analytical RP-HPLC confirmed that the purified MAX1 peptide was pure, the spectrum could not ascertain the identity of the pure species. In order to confirm that the purified peptide product was MAX1, the mass spectrum of the product was taken using ESI-MS. Pure MAX1 has an average molecular weight of 2229.9559g/mole. Figure 2.2 depicts a typical mass spectrum for pure MAX1. Due to the cleavage process and purification, nine TFA molecules were associated with MAX1 in its powder form. However, the electrospray ionization separated the TFA from MAX1, resulting in peaks for pure MAX1 plus two and three protons. The M+2H peak was 1115.4 mass to charge units as compared to the theoretical value of 1115.9 mass to charge units. Similarly, the M+3H peak was 744.2 mass to charge units, while the theoretical value was 744.3 mass to charge units. The M+3H peak was the predominate peak in the spectrum. These peaks, along with the absence of large unexpected peaks, indicated that the purified peptide had the same molecular weight as MAX1, and was therefore pure MAX1.

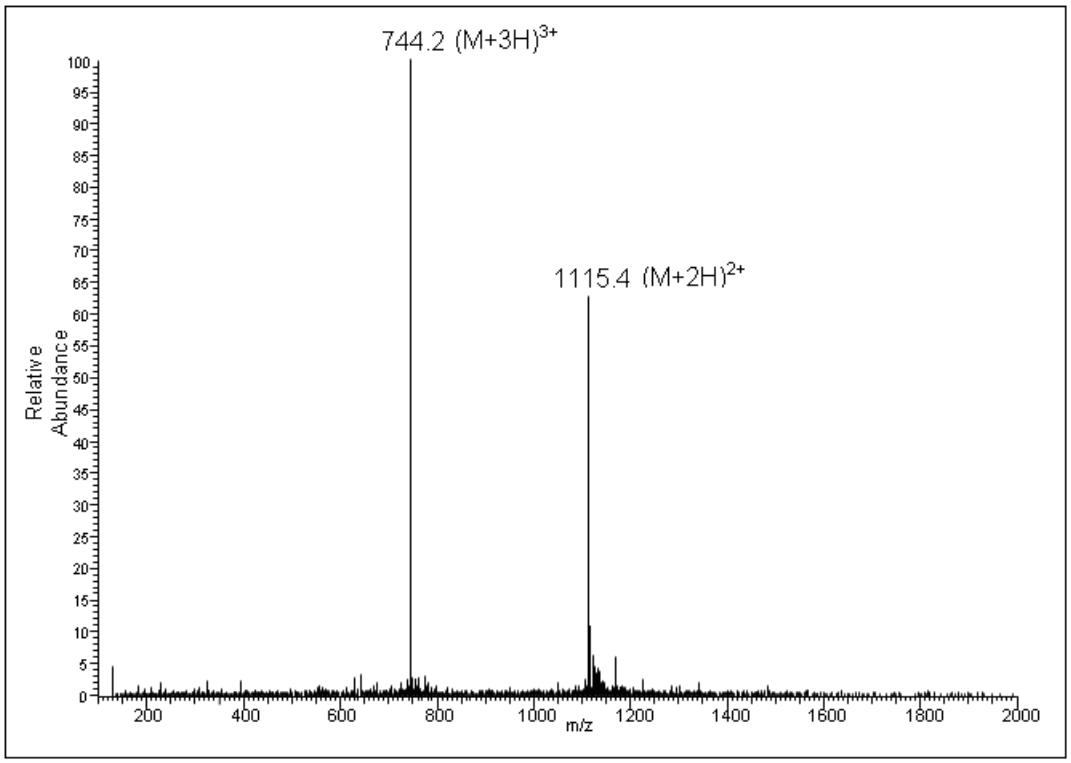

Figure 2.2 ESI-MS of pure MAX1. The M+2H and M+3H peaks were visible.

2.3.2 HPL1 Synthesis and Purification

Like MAX1, pure HPL1 was a white powder when lyophilized. The purity of the powder was determined using analytical RP-HPLC. Because HPL1 only differs from MAX1 by the length of the lysine side chains, the peptide charge was unaffected by the modification in the peptide sequence, and therefore the polarity of HPL1 was similar to that of MAX1. As with MAX1, HPL1 eluted as a sharp peak at approximately 28 minutes. Unlike MAX1, a small post-peak from 29 to 31 minutes was present in some purified samples. In cases where the post-peak was observed, the peptide sample in question was purified again with preparatory RP-HPLC using the

same gradient. The peptide was analyzed again using analytical RP-HPLC. In all cases, the post-peak disappeared after the second purification. Figure 2.3 shows an analytical RP-HPLC spectrum of pure HPL1.

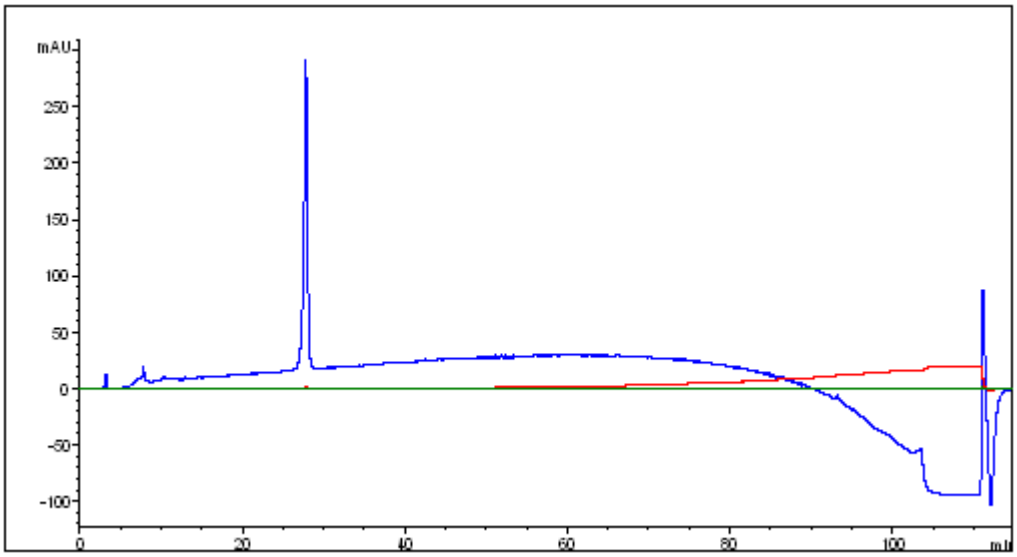

Figure 2.3 Analytical RP-HPLC of pure HPL1 in methanol. HPL1 eluted at 28 minutes.

Both MAX1 and HPL1 eluted at 28 minutes because they have the same polarity and are similar sizes. The purity of the HPL1 peptide powder was determined by ESI-MS. The average molecular weight of pure HPL1 is 2117.7192g/mole. Figure 2.4 presents a normal pure HPL1 mass spectrum. As with MAX1, the nine TFA molecules that normally associate with HPL1 were removed by electrospray ionization, resulting in three prominent peaks that correspond to pure HPL1 plus two, three, and four protons, respectively. The M+2H peak for HPL1 has a theoretical mass to charge ratio of 1059.9. The measured peak had a mass to charge ratio of 1059.3. Similarly, the M+3H peak was a mass to charge ratio of 706.7 and the theoretical

value was 706.9. For the M+4H peak, the mass to charge ratio was measured to be 530.3, while the theoretical value was 530.4. These peaks demonstrate that the peptide is pure HPL1, without any significant contamination from MAX1.

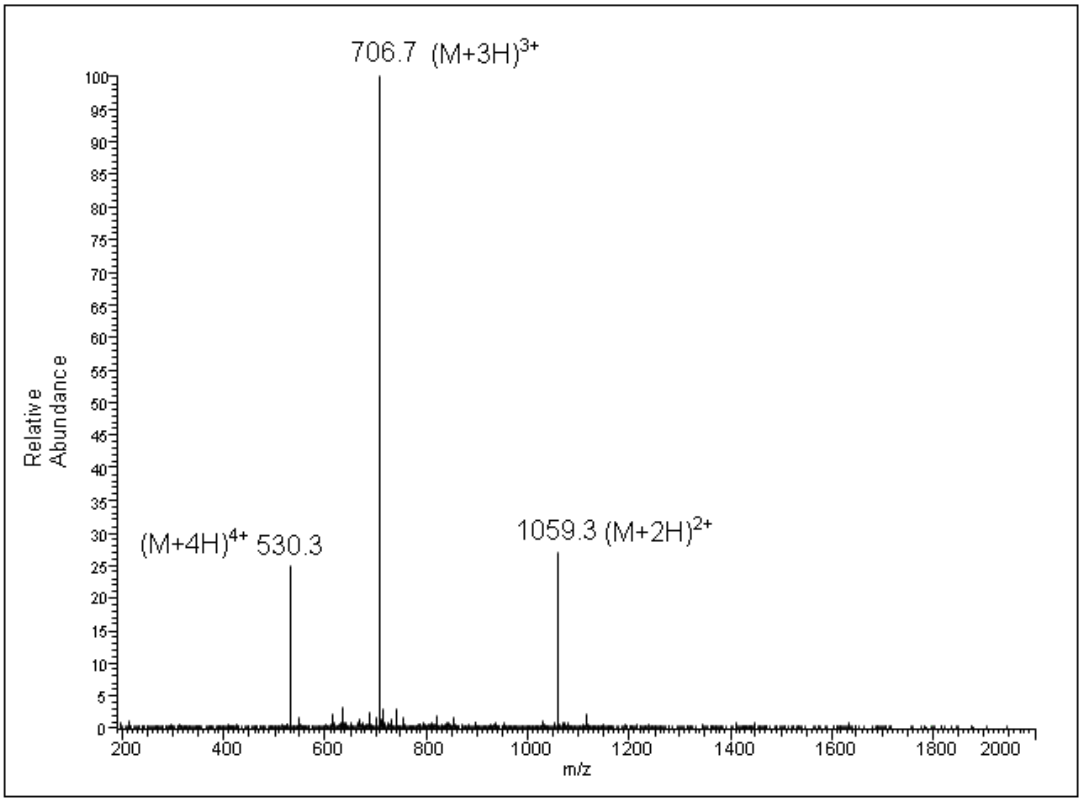

Figure 2.4 ESI-MS of pure HPL1. The M+2H, M+3H, and M+4H peaks were visible.

2.3.3 HPL2 Synthesis and Purification

As with MAX1 and HPL1, HPL2 was a white powder after being purified and lyophilized. The purity of the powder was determined by analytical RP-HPLC. A sharp peak in absorbance appeared at 28 minutes at 220nm. A smaller post-peak was also present between 29 and 31 minutes. The peptide was repurified three times using

preparatory RP-HPLC before the post-peak disappeared. The multiple repurifications of HPL2 resulted in a significant decrease in the yield of peptide. The pure HPL2 analytical RP-HPLC spectrum is shown in Figure 2.5.

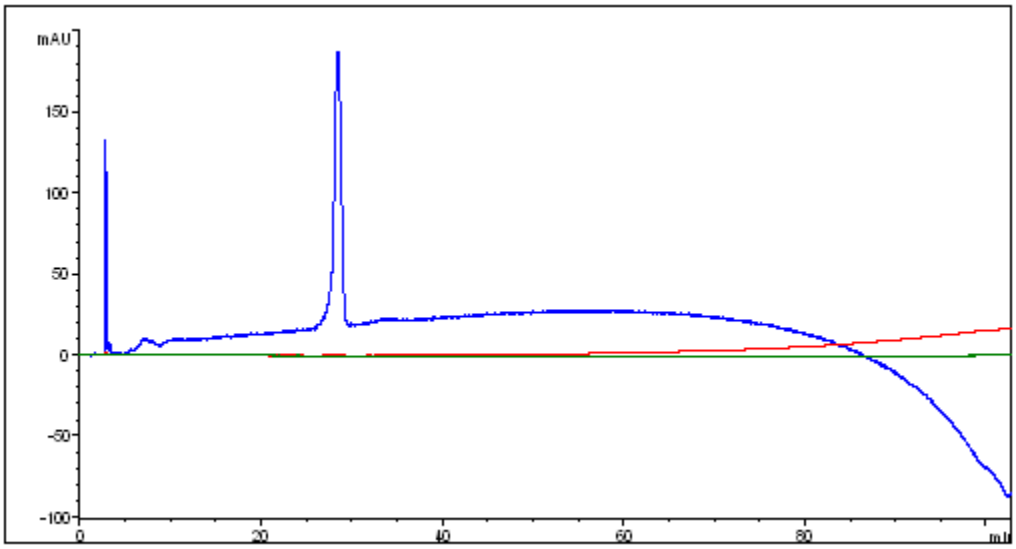

Figure 2.5 Analytical RP-HPLC of pure HPL2 in methanol. HPL2 eluted at 28 minutes.

The determination of the purity of the HPL2 peptide was dependent upon the mass spectrum since MAX1, HPL1, and HPL2 all eluted at 28 minutes. For HPL2, the average molecular weight was calculated to be 2005.5127g/mole. Figure 2.6 presents the best mass spectrum of HPL2. Many peaks are present, including the M+2H peak. The calculated mass to charge ratio for the M+2H peak was 1003.8, however the measured value was 1006.3. In addition to the small M+2H peak, there were several peaks for HPL2 associated with TFA. The predominant peak was at 299.9 mass to charge units, which corresponds to the peptide with nine protons and six TFA molecules, or theoretically a mass to charge ratio of 298.3. In each case, the

theoretical value was less than the value obtained from the ESI-MS spectrum. The deviations from the expected mass to charge ratios indicated that HPL2 was not fully purified.

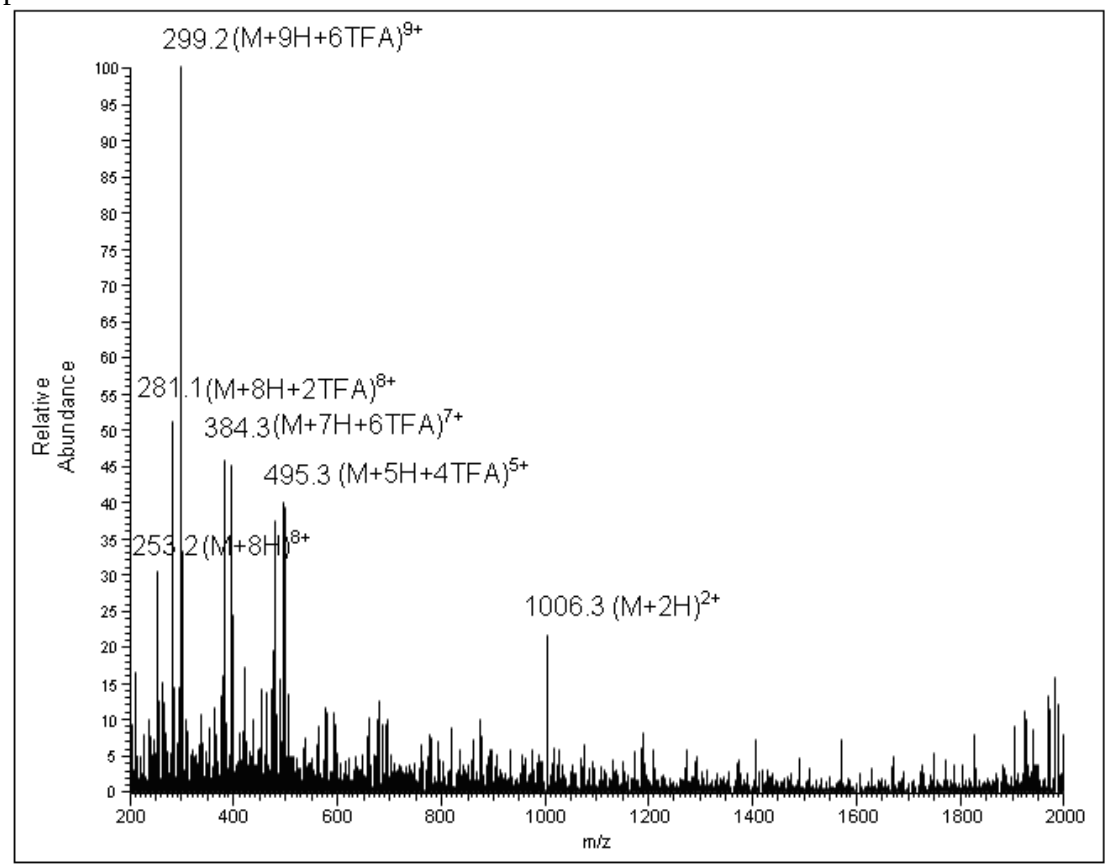

Figure 2.6 ESI-MS of pure HPL2. Several peaks are visible.

2.4 Conclusions

MAX1, HPL1, and HPL2 were synthesized on an automated ABI 433A peptide synthesizer employing standard Fmoc protocol and HCTU activation. After cleavage of the protecting groups and the resin, the peptides were purified using preparatory RP-HPLC. MAX1 was deemed pure using analytical RP-HPLC and ESI-

MS. However, HPL1 had a post-peak on its analytical RP-HPLC spectrum and required repurification in order to assure purity. For HPL2, the analytical RP-HPLC spectrum showed a post-peak that required three repurifications before it disappeared. The resulting mass spectrum of HPL2 showed that there were several deviations from the expected mass to charge ratios. This indicated that HPL2 was either not fully purified, or that some error had occurred in synthesis. Because of the expense of the diaminobutyric acid, HPL2 was not resynthesized.

Chapter 3

PHYSICAL PROPERTIES OF PEPTIDES

3.1 Introduction

In order to describe the physical properties of the peptides, oscillatory shear rheology and circular dichroism were used to quantify the rigidity of the hydrogel and the formation of beta sheets, respectively. Circular dichroism measures the amount of unfolded random coil peptide and folded peptide. By comparison, oscillatory shear rheology quantifies the beta sheet formation and the subsequent noncovalent crosslinking that result in the rigidity of the hydrogel. Using both techniques, the hydrogels were able to be fully characterized. For both HPL1 and HPL2, it was expected that beta sheets would remain the only type of coil because the sequence at the ß-type II turn was not modified for either peptide. However, it was expected that the change from lysine to ornithine would result in a decrease in the storage modulus due to a decrease in the non-covalent crosslinks. Less crosslinking would be expected because the decrease in side-chain length would result in a reduction in the entanglement, or facial packing deficits, of the beta sheet fibrils. A small decrease in the beta sheet formation, measured by the mean residue ellipticity, was also expected. Similarly, a more notable decrease was expected for HPL2, where lysine was replaced by diaminobutyric acid.

3.2 Materials and Methods

3.2.1 Materials

The serum-free Dulbecco's Modified Eagle's Medium (DMEM) and the S6 standard viscosity mineral oil were purchased from Sigma.

3.2.2 Oscillatory Shear Rheology

Experiments were performed on an AR 2000 oscillatory shear rheometer from TA Instruments with a 25mm-diameter stainless steel parallel plate geometry with a gap height of 0.5mm. Initially, a 4wt% peptide solution was formed by dissolving the peptide in 175μL of filtered H_2O. The solution was immediately diluted to a 2wt% peptide solution by adding 175μL of 1X DMEM. From the resulting solution, 300μL of the liquid were immediately transferred to a 10mm-diameter round mold with a parafilm base. The peptide solution in the mold was incubated at 37^{o}C for two hours. After two hours, 400μL of a 1:1 mixture of filtered H_2O and 1X DEMEM was gently added to the surface of the hydrogel. The hydrogel was returned to the incubator and incubated for an additional 22 hours. After a total of 24 hours of incubation at 37^{o}C, the hydrogel was gently transferred to the surface of the rheometer. To the edge of the steel plate, sufficient S6 standard viscosity mineral oil was added to ensure that the hydrogel was not in contact with the atmosphere. Measurements were taken at 37^{o}C. For the dynamic time sweep (DTS), the storage modulus (G') was monitored as a function of time over two hours with a frequency of 6rad/s and a strain of 0.2%. For the frequency sweep (FS), the storage modulus was monitored as a function of frequency, where frequency went from 0.1rad/s to 100rad/s with a strain of 0.2%. During the strain sweep (SS), the frequency was held constant at 6rad/s while the storage modulus was monitored as a function of percent strain, where the strain

went from 0.01% to 1000%. The reported storage modulus was the result of the average of three identically prepared samples with error shown.

3.2.3 Circular Dichroism

Circular dichroism (CD) measurements were made on a Jasco J-810 spectropolarimeter. A 2wt% stock solution of peptide was prepared by adding 100μL to the peptide and mixing. From the 2wt% stock solution, a 0.5 wt% peptide solution was prepared by adding 70μL of the 2wt% stock solution and 70μL of DMEM to the peptide and mix. From the resulting solution, 120μL was delivered to a 1μm cell. The mean residue ellipticity was monitored at 218nm for 2 hours at 37^{o}C. After 2 hours, a single measurement of the mean residue ellipticity was made from 200 to 260nm. The concentration of the solution added to the cell was determined by taking 20μL of the 2wt% peptide stock solution and adding it to 200μL of Standard A (99.9% filtered H_2O, 0.1% TFA). The resulting 20μL solution was added to 200μL of filtered H_2O. The absorption was measured on a Hewlett Packard 8453 UV-Visible Spectrophotometer at 220nm and the background region of 750nm to 800nm was subtracted to get the corrected absorption. The absorption coefficient for MAX1 is 15750$cm^{-1}M^{-1}$. It was assumed that HPL1 has an absorption coefficient similar to that of MAX1. The path length was 1cm. The reported mean residue ellipticity was the result of the average of three identically prepared samples with error shown.

3.3 Results and Discussion

3.3.1 Oscillatory Shear Rheology of Peptides

The viscoelastic behavior of the MAX1, HPL1, and HPL2 hydrogels were measured with oscillatory shear rheology. Originally, the storage and loss moduli of

the hydrogels were measured without an incubation period. For both HPL1 and HPL2, evaporation, marked by a sharp increase in the storage modulus, occurred because they become hydrogels slowly. Due to the slow hydrogelation of HPL1 and HPL2, the peptide hydrogels were incubated at 37^{o}C for 24 hours with a one to one mixture of filtered water and DMEM covering the hydrogels after two hours. This reduced the evaporation of the solution from the hydrogel while allowing the hydrogels to achieve a rigid state.

Figure 3.1 shows the dynamic time sweep of the 2wt% MAX1 hydrogel. It shows that initially the storage modulus, or elasticity, of the MAX1 hydrogel increased and then continued to slowly increase over time. The initial, steep increase in storage modulus was due to the transfer from the mold to the plate and the subsequent partial disruption of the self-assembled network in the hydrogel. Once the network recovers, the storage modulus continued to increase gradually. The continual rise in the storage modulus did not completely stop after two hours; however, it reached a relatively consistent value. At two hours, the storage modulus for 2wt% MAX1 was 4646±28 Pa. The loss modulus, also known as the viscosity, does not change significantly, as expected.

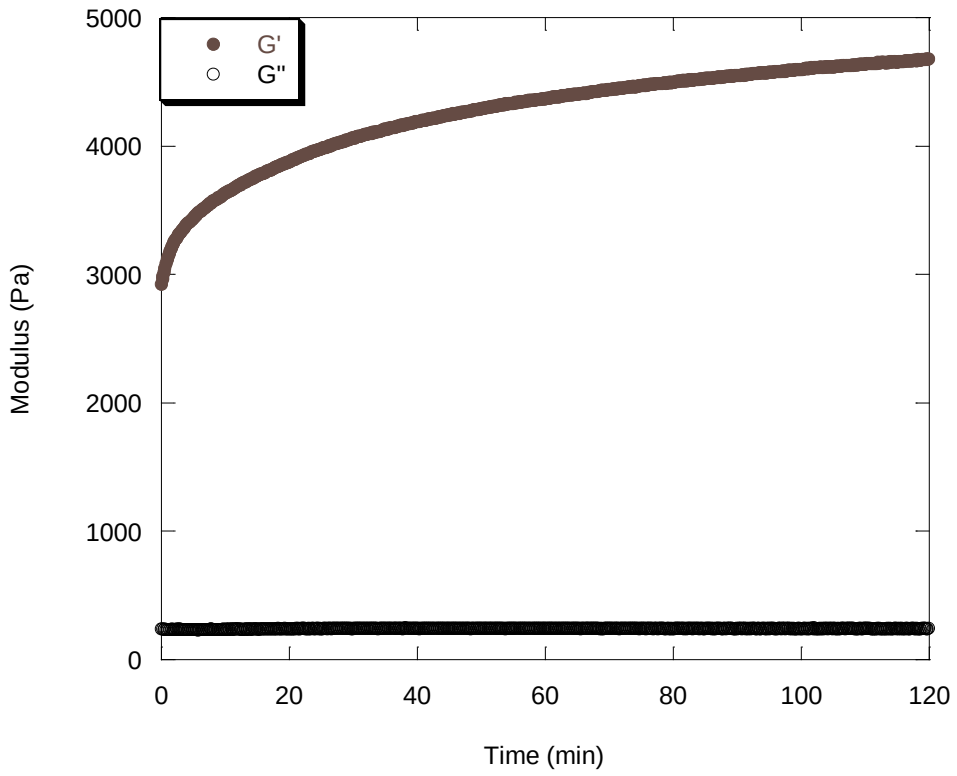

Figure 3.1 Dynamic Time Sweep measurements monitoring the evolution of the storage and loss moduli as a function of time for 2wt% MAX1 in DMEM after a 24 hour incubation period at 37^{o}C. G' is the storage modulus and G'' is the loss modulus.

After the dynamic type sweep, the 2wt% MAX1 hydrogel was exposed to a frequency sweep, as shown in Figure 3.2. During the frequency sweep, the storage and loss moduli are monitored with respect to an increasing frequency of tool rotation. The storage modulus of the hydrogel continued to increase slightly throughout the frequency sweep. The loss modulus fluctuated slightly because the hydrogel was slow to respond to the changes in frequency.

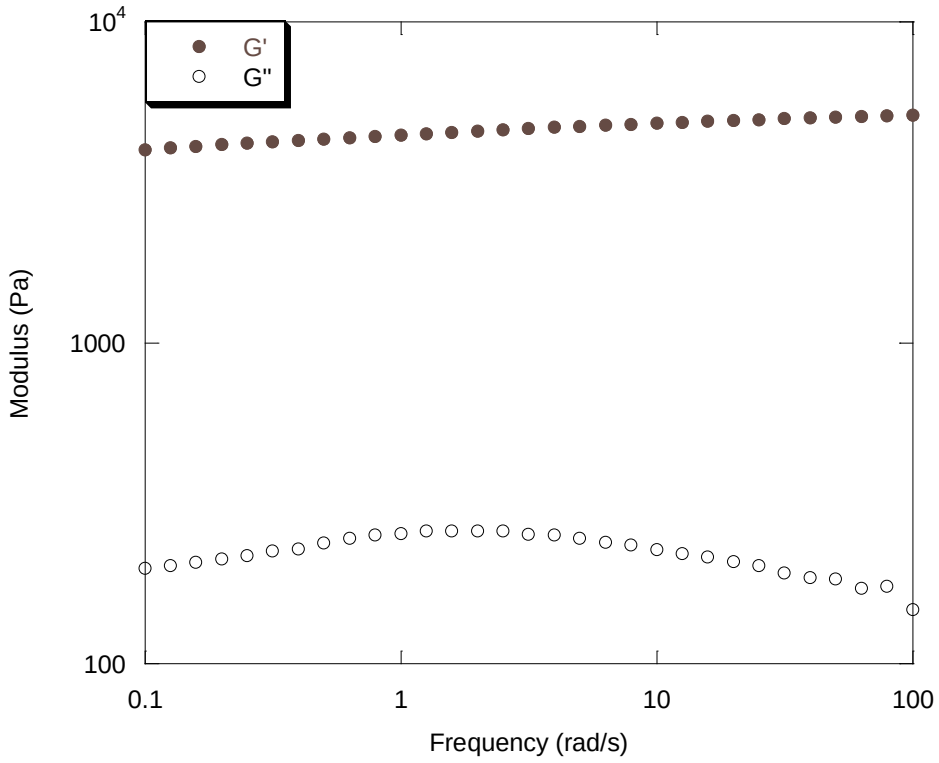

Figure 3.2 Frequency Sweep measurements monitoring the evolution of the storage and loss moduli as a function of frequency for 2wt% MAX1 in DMEM after a 24 hour incubation period at 37°C.

Figure 3.3 depicts the strain sweep for the 2wt% MAX1 hydrogel after the frequency sweep. For strain under 10%, the storage and loss moduli remained consistent; however after 10% strain the storage started decreasing significantly. There was a slight increase in the loss modulus after 10% strain, but the loss modulus quickly started decreasing. However, the loss modulus decreased less than the storage modulus and the loss modulus became larger than the storage modulus at strain larger than 27%. This indicates that under large amounts of strain the hydrogel returned to a

primarily liquid state and non-covalent crosslinks between the beta sheets were disrupted.

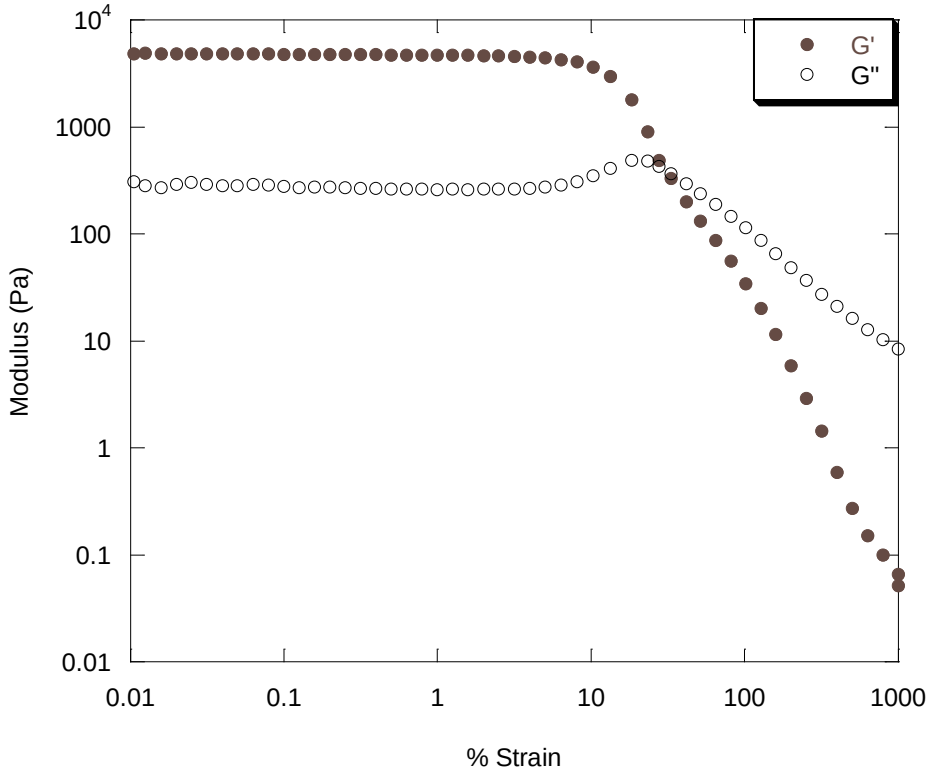

Figure 3.3 Strain Sweep measurements monitoring the evolution of the storage and loss moduli as a function of percent strain for 2wt% MAX1 in DMEM after a 24 hour incubation period at 37°C.

As with MAX1, oscillatory shear rheology was performed on HPL1 and the dynamic time sweep, frequency sweep, and strain sweep were measured. Figure 3.4 provides a representative dynamic time sweep of a 2wt% HPL1 hydrogel. As with MAX1, an initial sharp rise in storage modulus is followed by a gradually increasing storage modulus over time. However, the value of the storage modulus has been significantly decreased. The average storage modulus for a 2wt% HPL1 hydrogel was

755±132 Pa after two hours. This is a significant decrease in storage modulus when compared to 2wt% MAX1. The loss modulus did not change over the course of the dynamic time sweep and was consistent with the value obtained for the 2wt% MAX1 hydrogels.

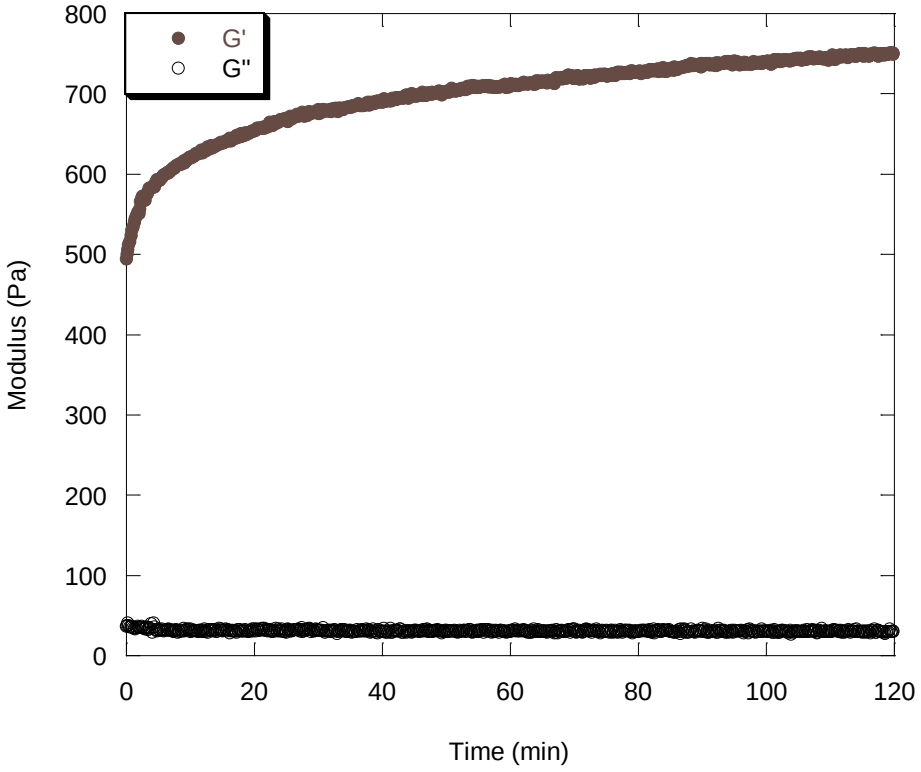

Figure 3.4 Dynamic Time Sweep measurements monitoring the evolution of the storage and loss moduli as a function of time for 2wt% HPL1 in DMEM after a 24 hour incubation period at 37^{o}C.

Figure 3.5 shows a typical frequency sweep for the 2wt% HPL1 hydrogels. As with MAX1, HPL1 showed a gradual increase in the storage modulus and fluctuations in the loss modulus. Additionally, as demonstrated by Figure 3.6, the storage and loss moduli of the 2wt% HPL1 hydrogel behaved similarly to that of the

2wt% MAX1 hydrogel. At strain above 27%, the storage modulus was less than the loss modulus.

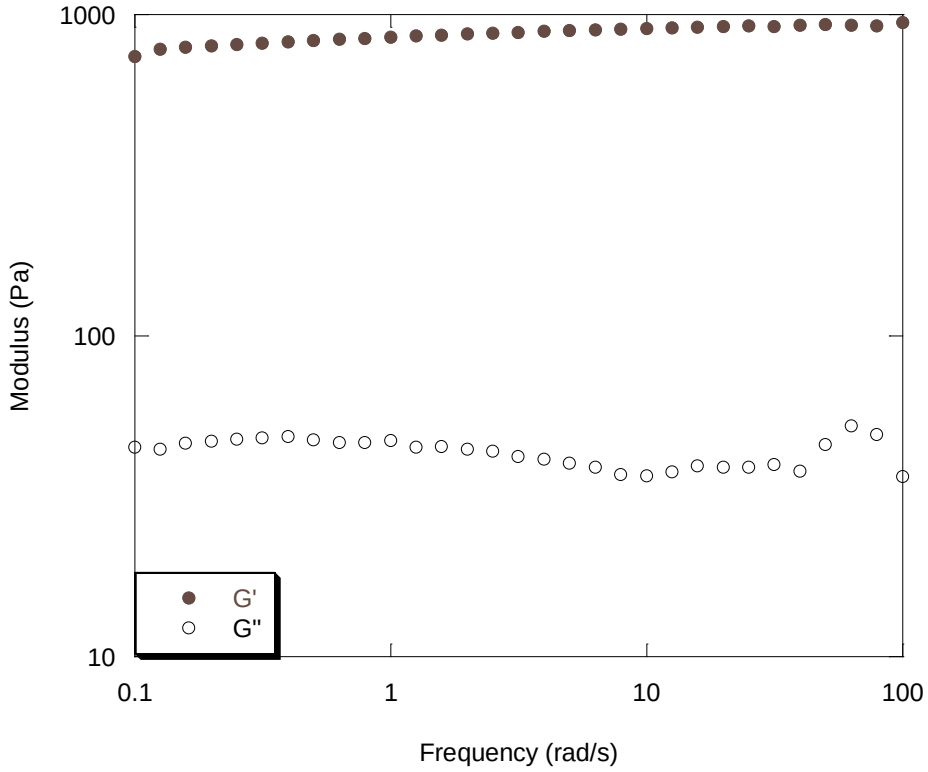

Figure 3.5 Frequency Sweep measurements monitoring the evolution of the storage and loss moduli as a function of frequency for 2wt% HPL1 in DMEM after a 24 hour incubation period at 37^{o}C.

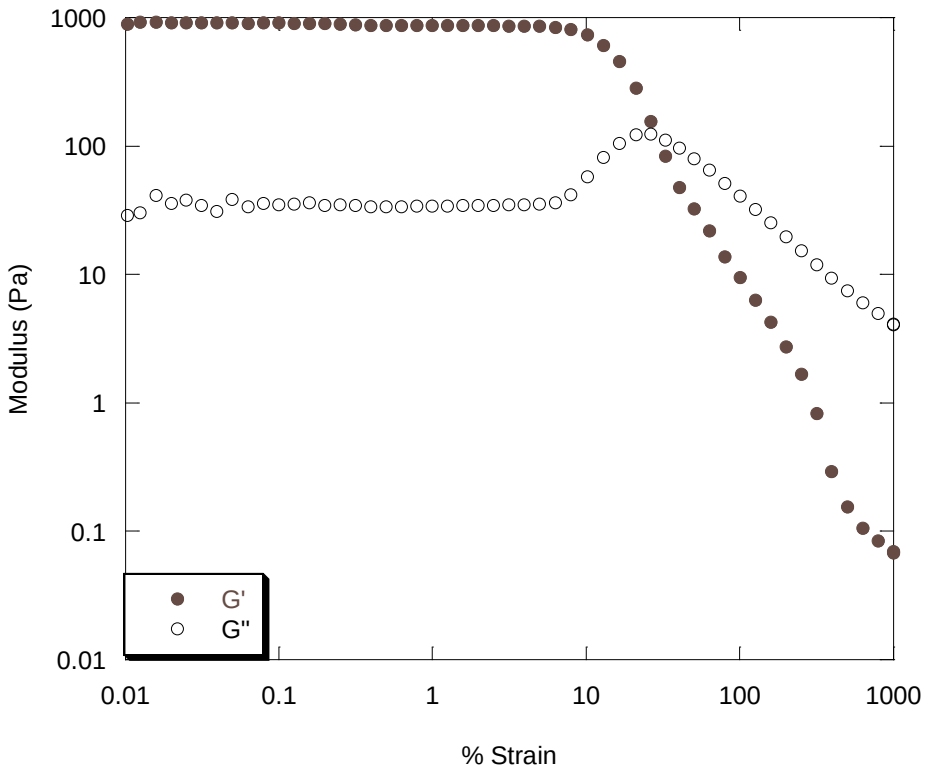

Figure 3.6 Strain Sweep measurements monitoring the evolution of the storage and loss moduli as a function of percent strain for 2wt% HPL1 in DMEM after a 24 hour incubation period at 37^{o}C.

Attempts to study 2wt% HPL2 failed because the hydrogel had not achieved a sufficiently rigid state after two hours of incubation. The gentle introduction of the one to one mixture of filtered water and DMEM to the surface of the 2wt% HPL2 hydrogel caused it to break into small hydrogel particles suspended in the solution.

3.3.2 Circular Dichroism of HPL1

Circular dichroism spectra of 0.5wt% MAX1 hydrogels showed a mean residue ellipticity minimum of -19×10^{3} deg·cm^{2}·dmol^{-1} at 216nm(14). Because of the

gelation kinetics, higher concentrations of peptide were not successfully studied. HPL1 was studied under the same conditions as the previous studies on MAX1. Figure 3.7 shows the gelation kinetics of 0.5wt% HPL1, where the mean residue ellipticity at 216nm was measured over a two hour period. At first there was a significant increase in the absolute mean residue ellipticity. This rate of increase in the absolute mean residue ellipticity slowed over time. This indicates that initially beta sheets are formed rapidly in the 0.5wt% HPL1 hydrogel, but over time the rate decreases. After two hours, 0.5wt% HPL1 was still slowly forming beta sheets.

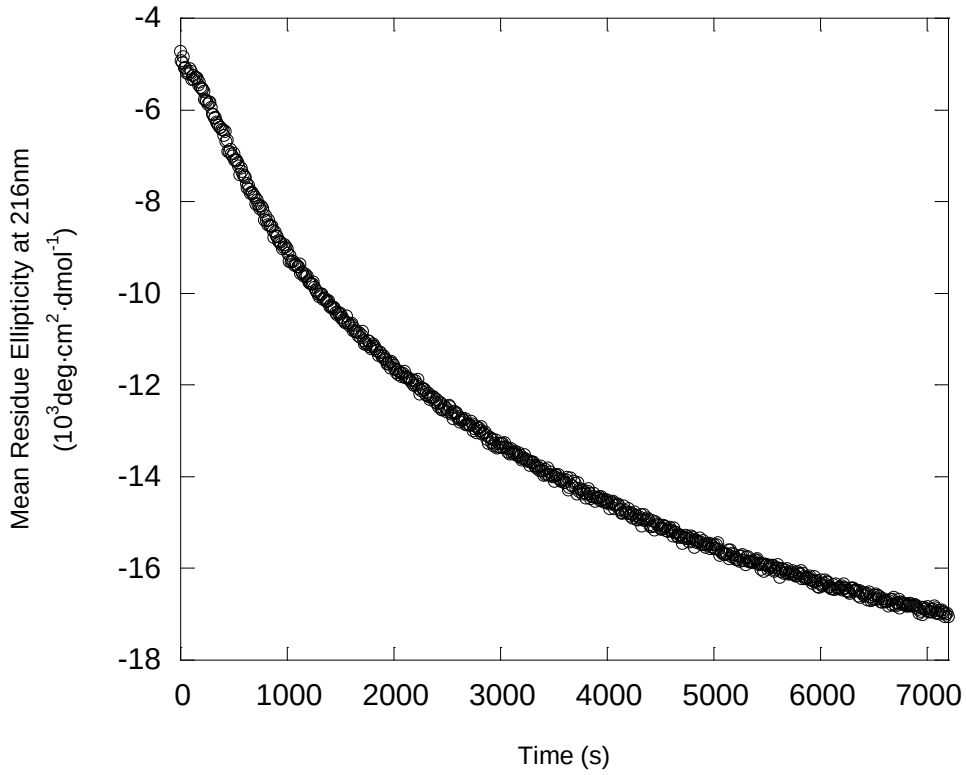

Figure 3.7 Mean Residue Ellipticity measurements as a function of time for 0.5wt% HPL1 in DMEM at 37^{o}C and 216nm.

Figure 3.8 depicts a wavelength spectrum of the same 0.5wt% HPL1 hydrogel after two hours at 37°C. As with the 0.5wt% MAX1 hydrogel, the minimum is at 216nm, indicating the formation of beta sheets. The average minimum mean residue ellipticity was -15521±53 deg·cm^2·dmol^{-1}, indicating a decrease in beta sheet formation. HPL2 was not studied under these conditions.

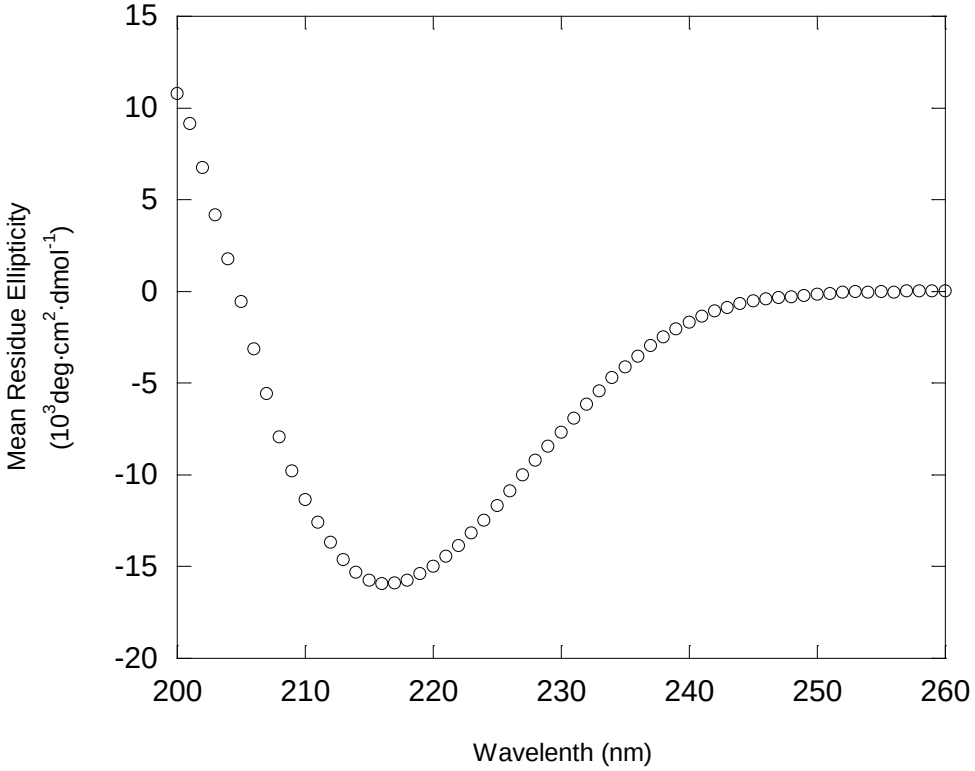

Figure 3.8 Mean Residue Ellipticity measurements as a function of wavelength for 0.5wt% HPL1 in DMEM after two hours at 37°C.

3.4 Conclusions

Preformed gels of 2wt% MAX1 and 2wt% HPL1 were studied using oscillatory shear rheology. MAX1 and HPL1 had storage moduli of 4646±28 Pa and

755±132 Pa, respectively, under the given conditions. Therefore, 2wt% MAX1 was over six times more rigid than 2wt% HPL1. HPL2 failed to form a sufficiently rigid hydrogel for study using oscillatory shear rheology. No further studies with HPL2 were pursued. Additionally, the beta sheet formation of 0.5wt% HPL1 was studied using circular dichroism. The HPL1 hydrogels had a relatively smaller mean residue ellipticity at 216nm than MAX1 hydrogels under the same conditions. This decrease could be due in part to the use of the absorptivity coefficient of MAX1 for HPL1. However, the difference in absorptivity coefficients would not be sufficient to solely account for the difference in mean residue ellipticities. Another possible reason for the decreased mean residue ellipticity was the fact that the 0.5wt% HPL1 hydrogel was still forming beta sheets after two hours and had not yet reached equilibrium, while similar MAX1 hydrogels were barely increasing in absolute mean residue ellipticity. Through oscillatory shear rheology and circular dichroism, it was shown that both MAX1 and HPL1 form rigid hydrogels where the main secondary structure is beta-sheet.

Chapter 4

ANTIBACTERIAL PROPERTIES OF HPL1

4.1 Introduction

Once it was demonstrated that HPL1 hydrogels had similar physical characteristics to MAX1 hydrogels and that 2wt% HPL1 hydrogels were sufficiently rigid to withstand the gentle introduction of a supernatant layer, the antibacterial properties of 2wt% HPL1 hydrogels were studied. In order to characterize the antibacterial activity of HPL1, 2wt% HPL1 hydrogels were exposed to concentrations of Gram-positive *Staphylococcus aureus* (*S.aureus*) and Gram-negative *Escherichia coli* (*E.coli*) ranging from 2×10^2 colony forming units (CFU)/ dm^2 to 2×10^9 CFU/dm^2. Both *S.aureus* and *E.coli* are both prevalent in hospital settings and were previously studied with 2wt% MAX1 hydrogels. Since a small amount of HPL1 peptide leeches from the hydrogel, the antibacterial properties of 100μM HPL1 soluble peptide solutions were studied when exposed to the same range of concentrations for the same bacteria species. As stated previously, 2wt% MAX1 hydrogels demonstrated broad spectrum antibacterial activity against *S.aureus* after 48 hours and antibacterial activity for concentrations of up to 2×10^6 CFU/dm^2 *E.coli*. Soluble 100μM MAX1 exhibited no antibacterial activity for both *S.aureus* and *E.coli* at all bacteria concentrations.

4.2 Materials and Methods

4.2.1 Materials

The Costar 96-well tissue culture treated polystyrene (TCTP) plates were purchased from Fischer. Trypic Soy Broth (TSB) was purchased from Bacto. The Trypticase Soy Agar plates with 5% sheep blood and powdered bacteria (*Staphylococcus aureus* and *Escherichia coli*) in separate vials were purchased from Becton Dickinson.

4.2.2 Antibacterial Assays

Hydrogels were prepared in separate wells of 96-well TCTP plates. A 4wt% HPL1 peptide stock solution was prepared by dissolving sufficient peptide in 875μL of filtered, sterile water. To each hydrogel well (wells B2 through D9), 35μL of 4 wt% peptide stock solution was added, followed by 35μL of DMEM. All pipetting was done slowly and carefully in order to prevent the formation of bubbles. The TCTP plate was covered and gently agitated without forming any bubbles. The resulting 2 wt% peptide hydrogels were incubated at 37^{o}C for 2 hours, at which time 200μL of DMEM was added. The gels were then allowed to equilibrate overnight at 37^{o}C.

The bacterial stock solution was prepared from powdered bacteria cultured on a Trypticase Soy Agar plate with 5% sheep blood at 37^{o}C. A colony from the fourth quadrant was transferred daily to a fresh agar plate, quadrant streaked, and incubated as above. To prepare the bacterial stock solution, one colony was taken from the fourth quadrant and suspended in 1mL of TSB. The resulting solution was gently agitated to ensure a homogenous solution. The optical density of the bacterial stock solution was adjusted to 0.1AU on a Hewlett Packard 8453 UV-Visible

Spectrophotometer employing a 1cm path length cell at 625nm by the addition of TSB, resulting in a 10^8 colony forming units (CFUs) per milliliter of bacterial stock solution. The resulting bacterial stock solution was used within ten minutes of preparation.

For each assay, the DMEM supernatant was removed from the gel and 100μL of TSB was gently added to the surface of each hydrogel, except for wells B9, C9, and D9. To these hydrogel surfaces, 111μL of the bacterial stock solution was added and 1:10 dilutions were performed across the plate, resulting in final bacterial concentrations of 2×10^2, 2×10^3, 2×10^4, 2×10^5, 2×10^6, 2×10^7, 2×10^8 and 2×10^9 CFU/dm^2, respectively, for each of the eight wells. Positive controls were performed on the TCTP surfaces (wells F2 through H9) using the same bacterial serial dilution as above. Negative controls were TSB on the TCTP surface (wells F12 to H12). Antibacterial assays were incubated for either 24 or 48 hours at 37^{o}C. After the appropriate time interval, the bacterial growth was monitored on a Hewlett Packard 8453 UV-Visible Spectrophotometer employing a 1cm path length cell by measuring the optical density at 625nm of the liquid above the gel by adding 100μL TSB to the surfaces, gently mixing, and transferring the supernatant to the cuvette. Corrected optical densities were calculated using the following equations:

$$CorrectedOD_{625nm} = 2\left(ObservedOD_{625nm} - \Delta OD_{1100nm}\right) \quad (1)$$

$$\Delta OD_{1100nm} = ObservedOD_{1100nm} - ExpectedOD_{1100nm} \quad (2)$$

$$ExpectedOD_{1100nm} = \frac{ObservedOD_{625nm}}{\left(\frac{OD_{625nm}}{OD_{1100nm}}\right)_{avg}} \quad (3)$$

The constant $\left(\frac{OD_{625nm}}{OD_{1100nm}}\right)_{avg}$ depends upon the bacterial species (*Escherichia coli*=3.37±0.02; *Staphylococcus aureus*=3.07±0.20). Each assay had three sets of serial dilutions. Final results represent triplicate, reproducible assays with the error shown.

4.2.3 Soluble Peptide Assays

The growth of *S. aureus* and *E.*coli in the presence of soluble HPL1 was measured using a broth dilution method. A 10^8CFU/mL stock solution in TSB was prepared as previously described. In a 96-well TCTP plate, 100μL aliquots of TSB was delivered to each of the wells from B2 through D8, F2 through H8, B12 through D 12, and F12 through H12, as with an antibacterial assay. To wells B9 to D9 and F9 to H9, 111μL of the bacteria stock solution were delivered and a 1:10 serial dilution was performed across the plate, resulting in final bacterial concentrations of 2×10^3, 2×10^4, 2×10^5, 2×10^6, 2×10^7, 2×10^8 and 2×10^9 CFU/dm^2, respectively. To wells B2 through D9 and B12 through D12, 10μL of a 1mM stock solution of HPL1 in water was introduced, resulting in a final concentration of 100μM HPL1. Samples were allowed to incubate for 24 hours at 37^{o}C. After 24 hours, the bacterial growth was monitored on a Hewlett Packard 8453 UV-Visible Spectrophotometer employing a 1cm path length cell by measuring the OD_{625nm} of the broth in each well by adding 100μL of bacteria-free TSB, gently mixing, and transferring the broth to a cuvette. Optical density calculations were performed using the same equations as shown for the antibacterial assays of the peptide hydrogels. The controls were bacteria in TSB, HPL1 in TSB, and TSB. Each assay had three sets of serial dilutions. Final results represent triplicate, reproducible assays with the error shown.

4.3 Results and Discussion

4.3.1 Antibacterial Assays of HPL1

In order to obtain preliminary data for 2wt% HPL1 hydrogels, antibacterial assays studying the antibacterial activity of 2wt% HPL1 against *Staphylococcus aureus* were performed for a 24 hour period. Figure 4.1 demonstrates the average antibacterial activity of 2wt% HPL1 after 24 hours. After 24 hours of exposure to *S.aureus*, the hydrogel demonstrated antibacterial properties for bacterial concentrations up to 2×10^{8} CFU/dm^2. However, uninhibited bacterial growth was observed for wells containing 2×10^{9}CFU/dm^2 of *S.aureus*. While not directly comparable, 2wt% MAX1 maintained antibacterial activity against equivalent bacterial concentrations for 48 hours (F). It could be expected that an increase in the incubation period for 2wt% HPL1 would result in a relative decrease of the antibacterial activity against *S.aureus*.

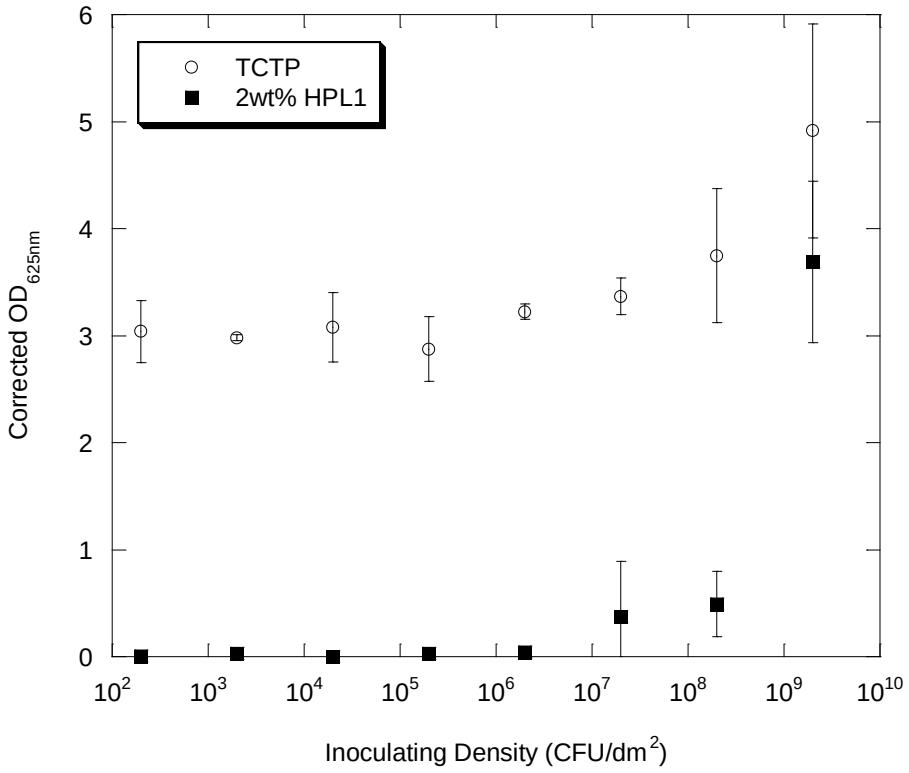

Figure 4.1 Antibacterial assay of 2wt% HPL1 challenged with increasing inoculating densities of *S.aureus* after a 24 hour incubation period. Control surfaces were Tissue Culture Treated Polystyrene (TCTP).

In addition to studying 2wt% HPL1 challenged with *S.aureus* for 24 hours, the hydrogels were examined for a 48 hour period. Figure 4.2 depicts the average antibacterial assay for the 2wt% HPL1 hydrogels that were challenged with *Staphylococcus aureus* for a period of 48 hours. As expected, the change from MAX1 to HPL1 and the incubation period of 48 hours resulted in a significant decrease in the antibacterial properties of the hydrogel. When compared to 2wt% MAX1 under similar conditions, 2wt% HPL1 maintained antibacterial activity for concentrations of up to 2×10^4 CFU/dm^2. At concentrations ranging from 2×10^5 CFU/dm^2 to

2×10^9CFU/dm^2, the 2wt% HPL1 demonstrated little to no antibacterial properties, whereas 2wt% MAX1 remained antibacterial (15).

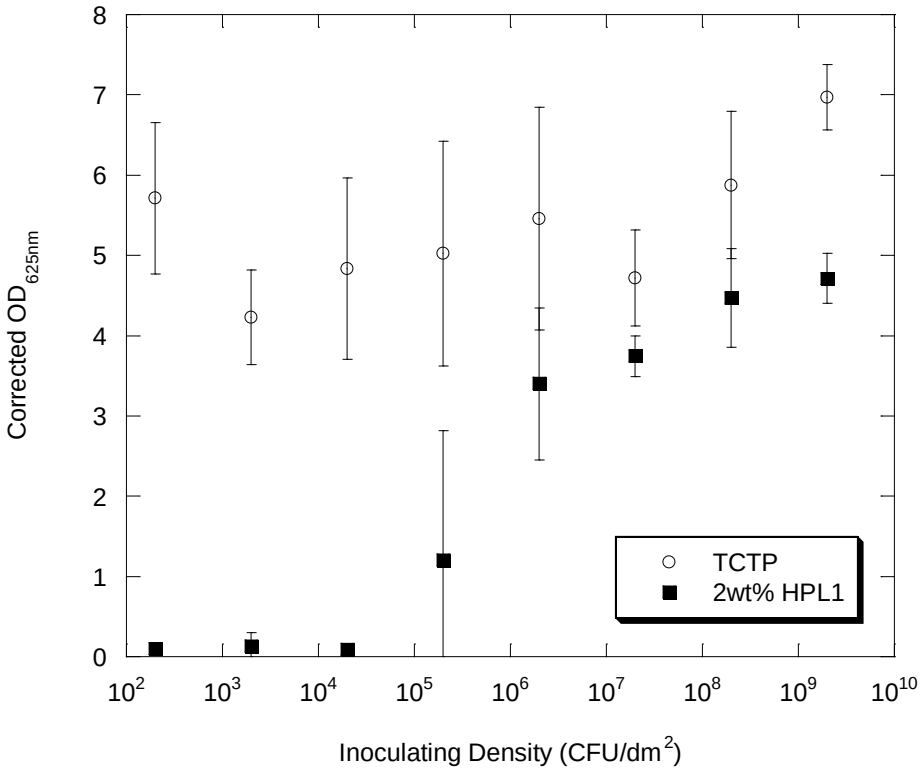

Figure 4.2 Antibacterial assay of 2wt% HPL1 challenged with increasing inoculating densities of *S.aureus* after a 48 hour incubation period. Control surfaces were Tissue Culture Treated Polystyrene (TCTP).

Figure 4.3 presents the antibacterial activity of 2wt% HPL1 exposed to *Escherichia coli* for a 48 hour period. After a two day period, the 2wt% HPL1 hydrogels demonstrated antibacterial properties across the entire bacteria concentration range. By comparison, 2wt% MAX1 demonstrated a loss of antibacterial activity starting at 2×10^7 CFU/dm^2 for *E.coli* (15). Therefore, 2wt% HPL1 has an increased antibacterial activity against Gram-negative *E.coli* when compared to 2wt% MAX1

under the same conditions. Since HPL1 demonstrated antibacterial properties across the entire range of concentrations of *E.coli* over a 48 hour period, 2wt% HPL1 was not studied for 24 hour periods.

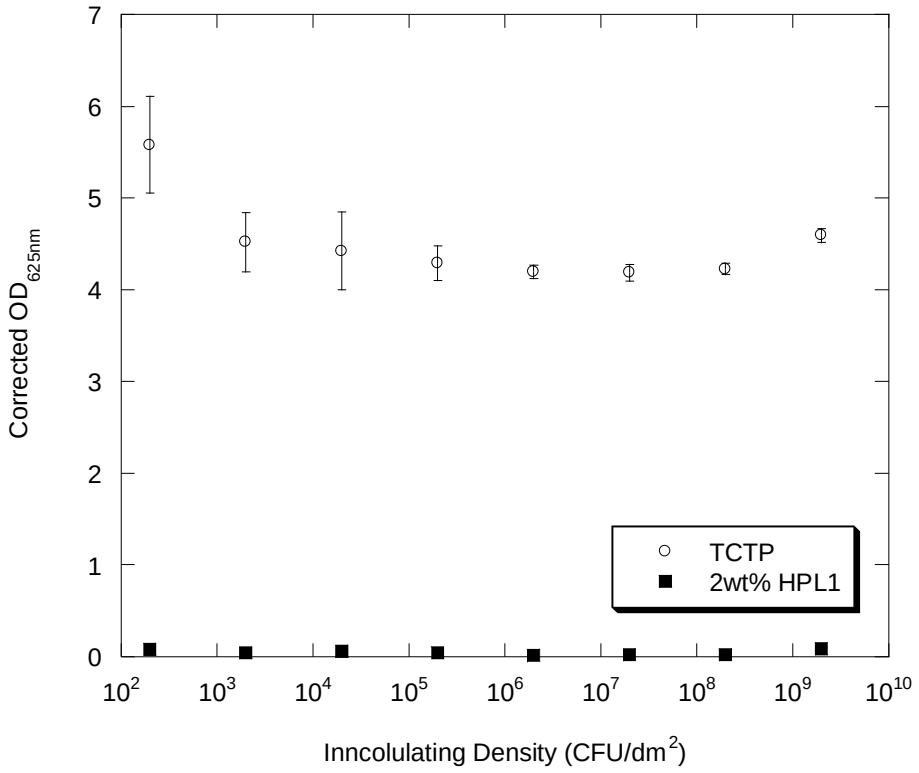

Figure 4.3 Antibacterial assay of 2wt% HPL1 challenged with increasing inoculating densities of *E.coli* after a 48 hour incubation period. Control surfaces were Tissue Culture Treated Polystyrene (TCTP).

4.3.2 Soluble HPL1 Assays

As with MAX1, it is possible that when HPL1 gels are initially formed, a small amount of the peptide that is in a folded state does not incorporate into the hydrogel and diffuses into solution. It is possible that the folded, soluble peptide, and not the hydrogel, is the antibacterial agent in the previous studies. In order to study

this possibility, the soluble peptide was studied at approximately three times the expected maximum concentration. Figure 4.4 depicts the soluble HPL1 peptide that was challenged with *S.aureus* for a 24 hour period. No antibacterial activity was observed for HPL1. This finding is consistent with that of MAX1.

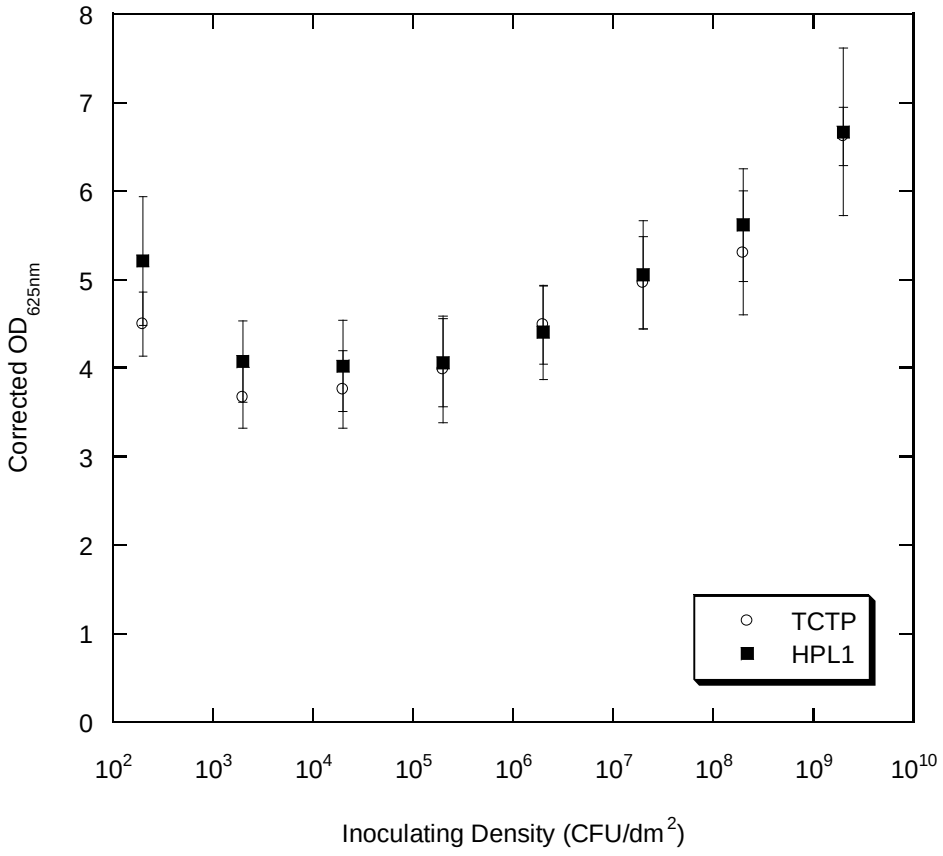

Figure 4.4 Soluble peptide assay of 100µM HPL1 challenged with increasing inoculating densities of *S.aureus* after a 24 hours incubation period. Control surfaces were Tissue Culture Treated Polystyrene (TCTP).

Similarly, Figure 4.5 shows 100µM HPL1 that was exposed to *E.coli* for a 24 hour period. Unlike the MAX1 observations, soluble HPL1 demonstrates some antibacterial activity at concentrations of *E.coli* less than 2×10^9 CFU/dm^2. While

2wt% HPL1 demonstrated antibacterial properties against all concentrations, it is possible that most of that activity was due to soluble, folded peptide that formed aggregates. However, because the 2wt% HPL1 hydrogel was antibacterial at 2×10^9 CFU/dm^2 for *E.coli*, it can be concluded that the gel also has some antibacterial activity. It should be noted that the absorbance of the soluble peptide alone had a corrected optical density of 0.68±0.07. Therefore, samples that demonstrated full antibacterial activity had absorbances above zero absorbance units.

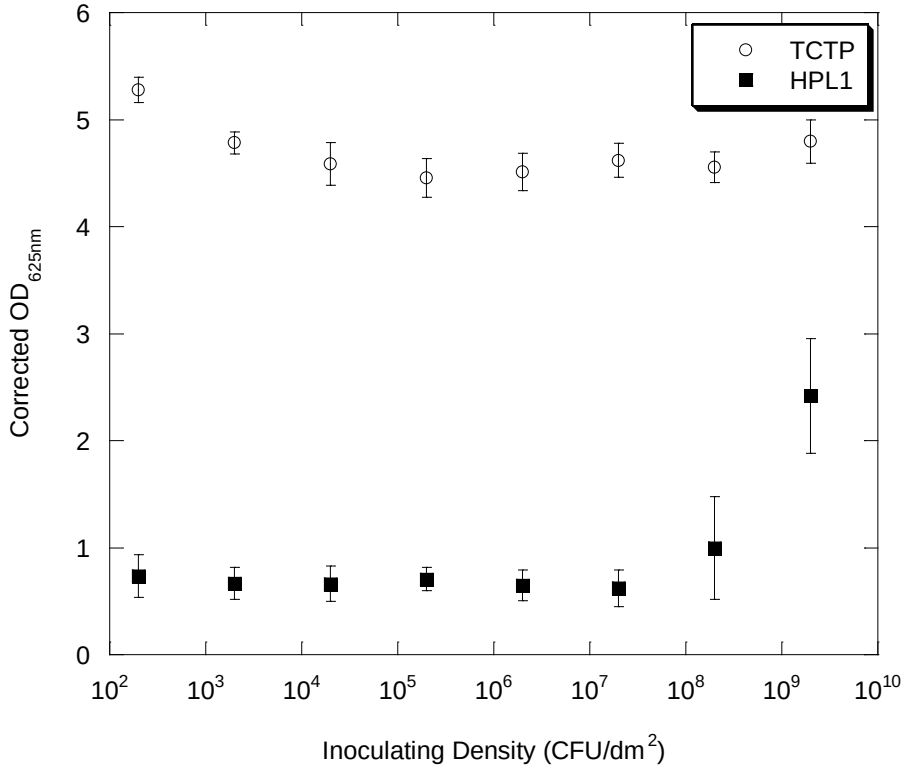

Figure 4.5 Soluble peptide assay of 100µM HPL1 challenged with increasing inoculating densities of *E.coli* after a 24 hours incubation period. Control surfaces were Tissue Culture Treated Polystyrene (TCTP).

Figure 4.6 presents the average corrected optical density for the control and HPL1 when exposed to 2×10^6 CFU/dm^2 bacterial concentrations. Unlike the similar MAX1 study where all optical densities were approximately the same, the optical density of soluble HPL1 exposed to *E.coli* showed a significant decrease. This indicates the antibacterial activity of 100μM HPL1 against *E.coli* is significantly greater than that of 100μM MAX1.

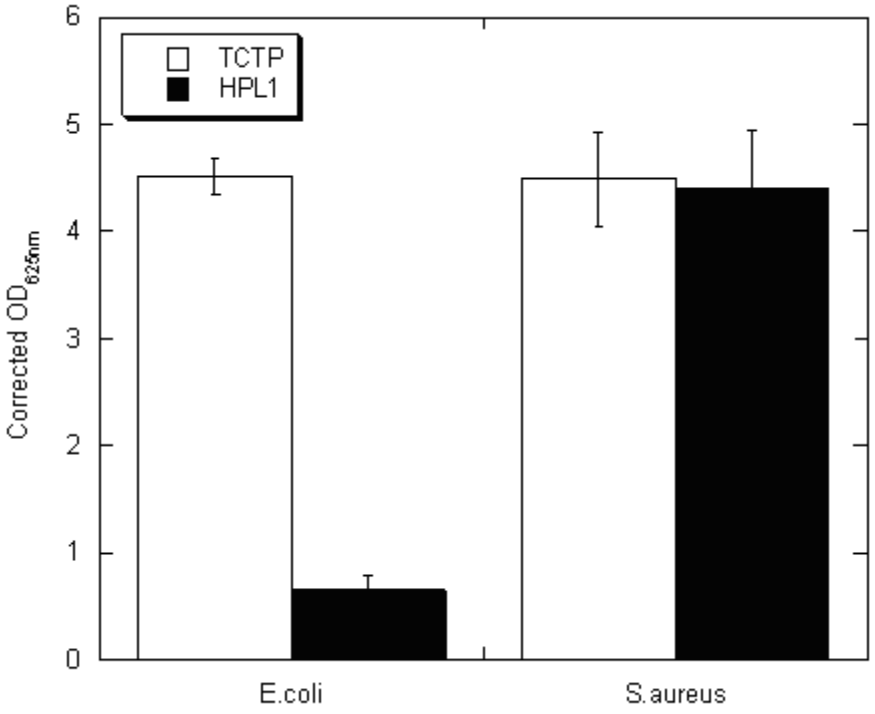

Figure 4.6 Soluble peptide assays of HPL1 for *E.coli* and *S.aureus* at an inoculating density of 2×10^6 CFU/dm^2. Control surfaces were Tissue Culture Treated Polystyrene (TCTP).

4.4 Conclusions

The antibacterial properties of HPL1 were studied both as a 2wt% gel and as a 100μM solution. As anticipated, for Gram-positive *Staphylococcus aureus*, the 2wt% HPL1 gels showed a loss in antibacterial activity at the highest inoculation density after a 24 hours incubation period. After a 48 hour incubation period, the 2wt% HPL1 hydrogels had lost antibacterial activity for concentrations above 2×10^4 CFU/dm^2 for *S.aureus*. By comparison, 2wt% MAX1 gels were antibacterial at all of the inoculating densities (15). The soluble 100μM HPL1 showed no antibacterial activity, as expected. However, the studies for Gram-negative *Escherichia coli* yielded unexpected results. After 48 hours of exposure to the inoculating densities of *E.coli*, the 2wt% HPL1 hydrogels inhibited bacterial growth in each sample. MAX1 under similar conditions displayed antibacterial activity for concentrations of *E.coli* for up to 2×10^7 CFU/dm^2 (15). When the soluble 100μM HPL1 was studied, it demonstrated antibacterial properties at all but the highest inoculating density. This result was unlike the results observed for soluble MAX1. Due to the results of the soluble peptide assays for HPL1, it cannot be definitively determined whether the 2wt% HPL1 gel had any antibacterial properties for Gram-negative species. A study using 2wt% HPL1 gels that were washed to remove any soluble aggregates of HPL1 would be necessary to study the antibacterial activity of the gel. Additionally, the results of the soluble HPL1 studies indicate the soluble HPL2 could possibly hold antibacterial activity against *E.coli* and other Gram-negative species.

Chapter 5

CONCLUSIONS

5.1 Conclusions

In summary, these experiments provide another clue as to the antibacterial mechanism of MAX1 hydrogels. By replacing lysine in the MAX1 sequence with ornithine and diaminobutyric acid to make HPL1 and HPL2, the role of the length of the lysine side chain was studied without altering the overall charge of the peptide. While HPL2 was difficult to purify and did not form a rigid hydrogel, HPL1 was able to be studied. It was demonstrated that the 2wt% HPL1 hydrogel had a storage modulus that was approximately six times less than 2wt% MAX1 formed under the same conditions. Additionally, beta sheet formation was slightly decreased in HPL1 when compared to MAX1. These changes in the physical properties were expected for HPL1.

In addition to the rheological and circular dichroism studies, antibacterial assays on the 2wt% HPL1 hydrogel and the soluble 100μM HPL1 were performed for *Staphylococcus aureus* and *Escherichia coli*. It was anticipated that a decrease in the length of the lysine side chain would result in a decrease in the antibacterial activity of the peptide because the amine groups are closer to the surface of they hydrogels and therefore not as capable of interacting with the bacterial membranes. As anticipated, the decrease in the length of the lysine side chain led to a decrease in the antibacterial activity of 2wt% HPL1 against Gram-positive *S.aureus*. The decrease in inhibition

was evident at the highest studied concentration after 24 hours and at concentrations above 2×10^4CFU/dm^2 after 48 hours. No antibacterial activity against *S.aureus* was observed for the soluble peptide. However, unexpected results were obtained for Gram-negative *E.coli*. The 2wt% HPL1 hydrogel demonstrated an increase in inhibition from 2×10^6 CFU/dm^2 for MAX1 hydrogels up to 2×10^9 CFU/dm^2 for HPL1. Moreover, unlike MAX1, the soluble HPL1 peptide showed antibacterial activity for *E.coli* for inoculations concentrations up to 2×10^8CFU/dm^2. While these results were unexpected, they provide some important insight into the mode of action of MAX1.

These results indicate that the length of the lysine side plays a role in the antibacterial mechanism of MAX1. The change from lysine to ornithine had opposite effects on Gram-positive and Gram-negative bacteria, in the former reducing antibacterial activity and in the latter increasing it. This suggests that the differences in cellular membranes have a role in the mechanism. It is likely that the lysine side chain enables the terminal amine to penetrate into the hydrophobic region of the outer membrane and competitively displace the divalent cations, calcium and magnesium, from the membrane. This would disrupt the membrane organization, increasing the permeability of the membrane. A possible explanation as to the difference in behavior between Gram-positive and Gram-negative bacteria lies in the difference in membranes. It has been suggested that relatively small peptides can sometimes pass through the outer membrane of Gram-negative species and then lyse the inner membrane. If the soluble HPL1 formed sufficiently small aggregates, or did not aggregate at all, it is possible that it could pass through the outer membrane of *E.coli* and interact with the inner membrane. It is even possible that MAX1 and HPL1 behave differently for Gram-positive and Gram-negative bacteria because they behave

using different mechanisms for the different classes. While it is not as likely, it is also possible that the MAX1 and HPL1 peptides interact and kill bacteria through target receptors.

5.2 Future Work

Further examination of MAX1 and HPL1 are necessary in order to obtain any definitive conclusions. The inhibitory role of the 2wt%HPL1 hydrogel in the absence of any soluble peptide should be determined for *Escherichia coli*. It is possible that the folded, soluble peptide, and not the surface of the hydrogel, is the primary antibacterial agent. Furthermore, *Staphylococcus aureus* and *Escherichia coli* were used as model Gram-positive and Gram-negative species. In order to make a generalization about the antibacterial activity of HPL1, and therefore MAX1, against a class of bacteria, more Gram-positive and Gram-negative species should be studied. In addition to the antibacterial assays, it would be interesting to perform live/dead laser scanning confocal microscopy (LSCM) on the 2wt% HPL1 and 100μM HPL1 soluble peptide that have been challenged with *E.coli*. It is possible that HPL1 merely inhibits the proliferation of *E.coli* as opposed to killing the organisms. Additionally, it would be of value to study the antibacterial activity of 100μM HPL1 soluble peptide against *E.coli*. Given the results of the soluble HPL1 studies, it is likely that soluble HPL2 possesses antibacterial properties against *E.coli*.

REFERENCES

1. Brogden, K. A. (2005). Antimicrobial peptides: pore formers or metabolic inhibitors in bacteria. *Nature Review Microbiology, 3*(3), 238-250.

2. Butler, D. L., Goldstein, S. A., & Guilak, F. (2000). Functional tissue engineering: the role of biomechanics. *Journal of Biomechanical Engineering, 122*(6), 570-575.

3. Dinh, S. M., & Liu, P. (Eds.). (2003). *Advances in controlled drug delivery: Science, technology, and products.* Washington, DC: American Chemical Society.

4. Drury, J. L., & Mooney, D. J. (2003). Hydrogels for tissue engineering: scaffold design variables and applications. *Biomaterials, 24*(24), 4337-4351.

5. Giuliani, A., Pirri, G., & Nicoletto, S. F. (2007). Antimicrobial peptides : an overview of a promising class of therapeutics. *Central European Journal of Biology, 2*(1), 1-33.

6. Hancock, R. E. & Rozek, A. (2001). Role of membranes in the activities of antimicrobial cationic peptides. *Federation of European Microbiological Societies Microbiology Letters, 206*(2), 142-149.

7. Kenawy, E. R., Worley, S. D., & Broughton, R. (2007). The chemistry and application of antimicrobial polymers: a state-of-the-art review. *Biomacromolecules, 8*(5), 1359-1384.

8. Kretsinger, J. K., Haines, L. A., Ozbas, B., Pochan, D. J., & Schneider, J. P. (2005). Cytocompatibility of self-assembled ß-hairpin peptide hydrogel surfaces. *Biomaterials, 26*(25), 5177-5186.

9. Mascaretti, O. A. (2003). *Bacteria versus antibacterial agents: An integrated approach*. Washington, DC: American Society for Microbiology Press.

10. Ottenbrite, R. M., Huang, S. J., Park, K. (Eds.). (1996). *Hydrogels and biodegradable polymers for bioapplications*. Washington, DC: American Chemical Society.

11. Ozbas, B., Kretsinger, J. K., Rajagopal, K., Schneider, J. P., & Pochan, D. J. (2004). Salt-triggered peptide folding and consequent self-assembly into hydrogels with tunable modulus. *Macromolecules, 37*(19), 7331-7337.

12. Pochan, D. J., Schneider, J. P., Kretsinger, J. K., Ozbas, B., Rajagopal, K., & Haines, L. A. (2003). Thermally reversible hydrogels via intramolecular folding and consequent self-assembly of a de novo designed peptide. *Journal of the American Chemical Society*, *125*(39), 11802-11803.

13. Ratner, B. D., Hoffman, A. S., Schoen, F. J., & Lemons, J. E. (Eds.). (1996). *Biomaterials science: An introduction to materials in medicine*. San Diego, CA: Academic Press.

14. Salick, D. A. (2009). Cytocompatibility, antibacterial activity and biodegradability of self-assembling ß-hairpin peptide-based hydrogels for tissue regenerative applications (Doctoral dissertation, University of Delaware, 2009).

15. Salick, D. A., Kretsinger, J. K., Pochan, D. J., & Schneider, J. P. (2007). Inherent antibacterial activity of a peptide-based ß-hairpin hydrogel. *Journal of the American Chemical Society, 129*(47), 14793-14799.

16. Schneider, J. P., Pochan, D. J., Bulent, O., Rajagopal, K., Pakstis, L., & Kretsinger, J. K. (2002). Responsive hydrogels from the intramolecular folding and self-assembly of a designed peptide. *Journal of the American Chemical Society, 124*(50), 15030-15037.

17. Shafer, W. M. (Ed.). (2006). *Antimicrobial peptides and human disease*. New York, NY: Springer.

18. Zasloff, M. (2002). Antimicrobial peptides of multicellular organisms. *Nature, 415*(6870), 389-395.